HOOP-WRAPPED, COMPOSITE, INTERNALLY PRESSURIZED CYLINDERS

Development and Application of a Design Theory

JOHN A WALTERS

Professional
Engineering
Publishing

Hoop-Wrapped, Composite, Internally Pressurized Cylinders

Development and Application of a Design Theory

by

John A Walters

Professional Engineering Publishing Limited
London and Bury St Edmunds, UK

First published 2003

ISBN 1 86058 425 X

A CIP catalogue record for this book is available from the British Library.

Typeset and Printed by J. W. Arrowsmith Ltd, Bristol

Related Titles of Interest

Title	Author	ISBN
Engineers' Guide to Pressure Equipment	C Matthews	1 86058 298 2
IMechE Engineers' Data Book: Second Edition	C Matthews	1 86058 248 6
Pressure Equipment Technology: Theory and Practice	Edited by W M Banks and D H Nash	1 86058 401 2
Guide to European Pressure Equipment	Edited by S Earland, D Nash, and B Garland	1 86058 345 8
International Conference on the Pressure Equipment Directive	IMechE Conference	1 86058 385 7

For the full range of titles published by Professional Engineering Publishing contact:

Marketing Department
Professional Engineering Publishing Limited
Northgate Avenue, Bury St Edmunds
Suffolk, IP32 6BW
UK
Tel: +44 (0)1284 763277 Fax: +44 (0)1284 718692
e-mail: marketing@pepublishing.com
Website: www.pepublishing.com

Contents

Foreword

It is hoped that the following design theory will be of use to those involved in the pressurized cylinders industry, and in particular to:

- Designers and manufacturers.
- Technical staff within user organizations.
- Inspection and testing bodies involved in product verification.
- Regulating bodies concerned with safety.

While the work is addressed to high-pressure gas cylinders in particular, it is equally applicable to other pressurized cylinders and pipes of similar transverse geometry and mechanical properties, subject to the same stress system.

Introduction

Over the past 30 years a broad technology has emerged using man-made high-strength fibres in engineering products. The trend started with the introduction of glass fibres, and was followed by aramids, and more recently by carbons. Restricted initial availability and high cost meant that early applications were limited to 'strategic' uses such as military and aerospace where high strength and low weight transcended other considerations.

As fibre availability increased other specialized fields of application have emerged, notably sporting goods, where in some cases the composite product is now the norm.

Less spectacularly, but nevertheless of both technological and commercial significance, high-strength fibres have become established in the field of high-pressure gas cylinder manufacture. As with other applications, fibres have made initial commercial impact in those cylinder uses where light weight is paramount, such as fire fighting and emergency rescue. This has been followed in other weight-sensitive products like portable medical cylinders and on-board tanks for containing the high-pressure gaseous 'alternative' clean burn automotive fuels compressed natural gas (CNG) and latterly hydrogen. While at the present time economic factors impede the widespread application of composite cylinders across the total range of compressed gases – and notably in the field of industrial gases – it seems certain that the growth trends observed over the past several decades will continue.

Composite cylinders fall into two basic types, namely, those which carry hoop-wrapped fibre reinforcement on

the cylindrical body part only, and those which carry a full hoop plus longitudinal body wrap including the cylinder ends. Of the two types, hoop-wrapped is the simpler, and is the subject of the following design theory.

The idea behind hoop-wrapping arises from the fact that in a conventional metallic cylinder the average body hoop stress is always twice that in the longitudinal direction. Thus the hoop direction is structurally the weak link, and will always be associated with a burst failure as caused by over-pressurization. By reinforcing the hoop direction the hoop/longitudinal stress ratio can be manipulated favourably, resulting in increased pressure containment capability. Furthermore, if the reinforcing medium is strong, stiff, and lightweight in comparison to the metallic body, the increased pressure capability will be accompanied by a corresponding improvement in cylinder gas containment to weight efficiency, which in the ideal condition could approach 100 percent, although in practice with real materials it will be less than this.

A feature of the hoop-wrapped cylinder is that over-reinforcement leads to a change in bursting from a hoop failure mode with longitudinal tearing of the body (as always occurs in an unwrapped cylinder) to a longitudinal failure mode with transverse fracture of the cross-section, resulting in the cylinder's separation and projection. This latter failure mode is, on safety grounds, considered unacceptable in most quarters. On the other hand, a cylinder carrying insufficient reinforcement will not fully exploit the potential gain offered by the hoop-wrapping process. It follows that a critical understanding of the factors influencing the change of burst mode is of importance to the design and manufacture of hoop-wrapped cylinders, and this aspect is a central part of the following design theory.

A further significant feature of hoop wrapping is that pre-stressing can be readily employed to provide favourable load sharing conditions between the metallic cylinder (or 'liner' as it is called) and the fibre/resin overwrap. While not affecting ultimate bursting conditions, pre-stressing can significantly improve cyclic fatigue performance of the 'liner' by reducing tensile hoop stress in the normal elastic operating range. A convenient method of imparting pre-stress is by autofrettaging the wrapped cylinder, involving deliberate over-pressurization into the metallic liner's plastic range during manufacture. A quantitative understanding of the relationship between autofrettaging pressure and resulting pre-stresses in liner and fibre is important, and accordingly is comprehensively treated in the following theory.

Although the hoop-wrapped cylinder is the simplest and heaviest of the composites, it has and will continue to have an important role in the compressed gas industry. It represents a link between the traditional all-metal cylinder and the avant-garde sophisticated fully wrapped types, in that the 'liner' of the hoop-wrapped cylinder remains a major load-bearing structural feature of the overall cylinder design. While weight saving is less than with full wrapping, it is nevertheless very significant compared with what is possible by metallic pressure vessel materials development. Furthermore, whatever may occur in the latter can always be augmented by fibre hoop wrapping. Other important techno-economic aspects of the hoop-wrapped cylinder are:

- The geometry of the liner often remains within the range of the all-metal equivalent cylinder, and therefore existing well-proven production plant and processes can be utilized for liner production.

- Fibre is expensive, and the hoop-wrapped cylinder uses considerably less fibre than its fully wrapped counterparts.
- Because a higher proportion of the working pressure load is carried by the liner, a hoop-wrapped cylinder is arguably more damage tolerant than a fully wrapped cylinder.

It is believed that the above points support the case for improving the technological design basis of the hoop-wrapped cylinder.

Present state of the art

As manufacturing techniques and markets for composite cylinders have developed, a need has arisen for product standards, first at national level, then at regional level, and ultimately at international level. Examples of these, respectively are: in the USA, Department of Transportation (DOT) (**1**) and in the UK, Health and Safety Executive (HSE) (**2,3**) specifications; EN European Standards (**4**) for reference in European Road/Rail Transport Regulations (ADR/RID); and ISO Standards (**5**) for reference in United Nations (UN) Transport Regulations. The American Society of Mechanical Engineers (ASME) has recently published a Code Case covering design requirements for large, transportable, hoop-wrapped cylindrical pressure vessels (**6**).

Since composite cylinders are often used in the same markets and for the same purpose as traditional all-metal cylinders, standards for composites are intended to provide the same overall level of safety, and as far as possible are written in a similar way - but with one important exception, namely, the approach to cylinder design. With metallic cylinders it has been the long-held practice to provide in the standard a specific clause on design including stress formulae derived from well-established materials theory. This approach is unambiguous, ensuring that the stress in the body of the cylinder due to internal pressurization never exceeds a given safe proportion of the material's strength properties under normal operating conditions. However, with the greater complexity of composite cylinders it has generally been

judged too difficult to follow a similar track. Instead, the concept of 'performance-based' design has been introduced whereby the adequacy of a new cylinder is proven by carefully selected tests intended to represent extremes of service conditions.

Although this essentially experimental 'performance-based' approach to design leads to a safe composite cylinder, it is inevitably resource consuming and costly in the amount of testing required compared with prescriptive design; while it may be the most suitable (indeed only) course with an infant technology, there is a strong case, as the technology develops, to graduate into predictive design, thereby reducing the test burden and introducing a common, transparent, approach available to all concerned. It goes without saying that such a move requires provision of accurate, reliable design theory.

Even in the present state of the art, where performance testing is the norm, it is a fact that regulating bodies in several prominent industrialized countries insist on a design assessment by the composite cylinder manufacturer as part of the Approval procedure. At present this requirement is met by employing proprietary computer programmes using numerical modelling techniques to optimize prescribed concurrent conditions for a particular cylinder, in the form of a design statement. The approach falls short of revealing the relative influence of the design variables as would be provided by a general theory, but is probably useful in the absence of the latter, if only to demonstrate that the manufacturer is applying more than just experimental methods. However, some camps reject the mathematical modelling approach to design as part of Approval on the basis that calculation results cannot be independently checked, and therefore add no value to the performance testing already required.

The foregoing makes a powerful argument for an accurate theoretical approach to composite cylinder design – where/when such is possible. Work carried out by the author, as documented in the following exposition, shows that a comprehensive theoretical treatment of design is possible in the case of the hoop-wrapped cylinder, and it is believed that considerable benefits to the compressed gases industry, in terms of safety, technical optimization, and economies of manufacture, will result from its application.

Although no broad theoretical design philosophy has hitherto existed for hoop-wrapped composite cylinders, design 'tools' in the form of optimization software programmes have been developed, and are used privately by manufacturers. The best known of the early versions was that by NASA (**7**), licensed to several North American cylinder makers. More recently a paper by researchers at Alcoa (**8**) provides insight into the numerical optimization approach as applied to a particular aluminium/glass design. It is claimed by the authors of the paper that the developed mathematical model is an advance on NASA, and from presented results the model appears to give reasonable agreement with experimental data, except in the case of predicting the burst mode transition. The Alcoa paper makes a significant contribution, not least for the amount of experimental information contained, which, it is acknowledged, has been used in comparing results predicted by the following theory.

References

(1) DOT FRP-2 Standard: *Basic requirements for fibre reinforced plastic (FRP) type 3HW composite cylinders* (1987 revision).

(2) HSE-AL-HW1: *Specification for hoop wrapped composite aluminium alloy gas cylinders* (1994).

(3) HSE-SS-HW3: *Specification for hoop wrapped composite seamless steel gas cylinders* (1997).

(4) EN 12257: *Transportable gas cylinders – Seamless, hoop wrapped composite cylinders* (2002).

(5) ISO 11119-1: *Gas cylinders of composite construction – Specification and test methods – Part 1: Hoop wrapped composite gas cylinders* (2002).

(6) Code Case 2390, *Composite reinforced pressure vessels*, Section VIII, Division 3 of ASME Boiler and Pressure Vessel Code (2001), American Society of Mechanical Engineers, New York.

(7) **Johns, R.H.** and **Kaufman, A.** NASA TMX-52171, Lewis Research Centre (1964).

(8) **Teply, J.L.** and **Herbein, W.C.** Failure modes for filament wound aluminium natural gas cylinders (Alcoa Labs, Alcoa Center, Pennsylvania). Paper presented at an ASM International Conference on *Fatigue, Corrosion Cracking, Fracture Mechanics and Failure Analysis*, Salt Lake City, Utah, USA, December 1985.

Part 1

Development of the theory

The following general points are made in setting the scene.

Compared with an all-metal cylinder, a composite cylinder – even a relatively simple hoop-wrapped type – presents a more complex design problem. Not only are there more variables to be considered, but an understanding of the interaction between the liner and overwrap is crucial to the understanding of the cylinder's overall behaviour as a pressure vessel. The principal objective of the following analyses is to provide engineers with a comprehensive, philosophical framework for the design of hoop-wrapped composite gas cylinders, taking account of all important design variables and their interactions. The approach followed throughout has been to link cause and effect in the form of explicit mathematical formulae, capable of solution by traditional methods without recourse to computer numerical techniques, although the user may choose to computerize parts of the procedure to reduce the calculation burden. However, the real value of the approach is in revealing the fundamental nature of cause and effect, and the importance of this should not be lost in the calculation process.

During normal use a hoop-wrapped composite gas cylinder is designed to operate as an elastic body, such that repeated pressurization and emptying produces no permanent strain. However, a method often used to increase the elastic range in service is to produce controlled plastic overstrain in the liner during cylinder manufacture. Furthermore, burst characteristics of the cylinder are intimately associated with plastic deformation of the liner. Without exaggeration, consideration of the plastic

behaviour of the liner in the presence of elastic constraint of the reinforcing overwrap has provided *the essential insight necessary for developing the following design theory.*

Although the composite overwrap comprises two components, i.e. fibre and resin matrix, the latter is of low tensile modulus and strength compared with the entrapped continuous fibres. For example, of the commonly used fibres, i.e. glass, aramid and carbon, glass with the lowest modulus of the three is 30 times stiffer than epoxy resin, and the strength of all of these fibres exceeds the resin by at least 40 times. Therefore, although the matrix positions the continuous fibres to the hoop pressure load, it makes little contribution to the structural strength of the cylinder, and for that reason in developing the theory a simplifying assumption has been made of a liner overwound only with high-strength fibres of mechanical properties as measured in the resin-impregnated, cured condition. This has the further advantage that the theory is concerned only with the amount of reinforcing fibre required, the mix of fibre/resin volume actually used in manufacture being a separate non-essential issue, and any slight theoretical error arising will be on the conservative side.

1.1 Notation

a	Area, generally
a_{ci}	Effective liner/overwrap interface hoop load area per unit longitudinal length ($= D$)
a_{c0}	Effective internal hoop pressure load area per unit longitudinal length ($= d$)
a_f	Total hoop cross-sectional area of fibre per unit longitudinal length (i.e. both sides)

a_{fc}	Total *critical* hoop cross-sectional area of fibre per unit longitudinal length (i.e. both sides)
a_{fd}	Total *design* hoop cross-sectional area of fibre per unit longitudinal length (i.e. both sides)
a_θ	Total hoop cross-sectional area of liner wall per unit longitudinal length ($= 2t$ both sides)
A	Liner geometry coefficient t/D
d	Internal diameter of liner
D	External diameter of liner
E_f	Tensile modulus of fibre
E_l	Tensile modulus of liner
FSR	Fibre stress ratio (as defined in Section 1.6.3)
K	Liner geometry coefficient $d^2/(D^2 - d^2)$
l	General suffix denoting longitudinal direction (e.g. of stress)
m	Cylinder burst coefficient (as defined in Sections 1.4 and 1.5)
n	Cylinder burst coefficient (as defined in Sections 1.4 and 1.5)
p	Pressure, generally
p_a	Autofrettage pressure
p_b	Burst pressure
p_{bc}	Critical burst pressure
p_{bd}	Design burst pressure
p_{bl}	Liner burst pressure (without overwrap)
p_{br}	Required minimum burst pressure
p_d	Design pressure associated with FSR
p_h	Hydrostatic test pressure
p_i	Liner/overwrap interface pressure
p_s	Service pressure
p_{y0}	Initial yield pressure of hoop-wrapped liner
r	General suffix denoting radial direction (e.g. of stress)
t	Wall thickness of liner cylindrical body
T_f	Tensile strength of resin-impregnated fibre strand
T_l	Tensile strength of liner
X	Fibre stress coefficient (as defined in Section 1.6.3)
Y	Current yield stress of liner

Y_m Mean liner yield stress over a specified strain increment
Y_0 Initial yield stress of liner prior to autofrettage
Z Liner hoop stress coefficient (as defined in Sections 1.6.1 and 1.6.2)

δ General prefix denoting an increment (e.g. of strain)
δD Diametrical permanent expansion in autofrettage
ε Strain, generally
ε_e Equivalent strain in liner
ε_f Strain in fibre
ε_l Longitudinal strain in liner
ε_θ Hoop strain in liner
θ General suffix denoting hoop direction (e.g. of stress)
ν Poisson's ratio
σ Stress, generally
σ_e von Mises equivalent stress in liner
σ_f Fibre stress
σ_{fd} Fibre design stress associated with FSR
σ_{f0} Fibre pre-stress after autofrettage
σ_l Longitudinal stress in liner
σ_m Denotes a mean principal stress in liner over a specified strain increment
σ_r Mean radial stress in liner wall
σ_θ Hoop stress in liner
$\sigma_{\theta 0}$ Liner hoop pre-stress after autofrettage
σ' Denotes a deviatoric stress in liner

1.2 Characterization of cylinder behaviour under pressure

Figure 1.1a shows a cross-section of a typical hoop-wrapped gas cylinder, including an inset three-dimensional segment of the cylinder wall. Figure 1.1b is an enlarged view of the segment showing liner principal stresses σ_θ, σ_l,

and σ_r, and fibre stress σ_f. Generally σ_l and σ_θ will be large compared with internal pressure p and mean wall radial stress σ_r, and therefore the liner approaches a condition of plane stress. However, as will be shown later, this does not a priori justify the blanket assumption of plane stress for all combinations of liner and fibre, but it *does* provide a useful analogy for visualizing stress patterns in the liner (and by implication in the fibre) at various stages of pressurization as shown below.

For plane stress (with $\sigma_r = 0$) the von Mises yield criterion reduces to

$$Y^2 = \sigma_\theta^2 + \sigma_l^2 - \sigma_\theta \cdot \sigma_l$$

which plots as an elliptical locus in the principal stress plane. Figure 1.1c shows this locus in the positive stress quadrant typical of a pressurized cylinder. Any point on the locus represents a σ_l, σ_θ condition causing yielding at yield stress Y, whereas all σ_l, σ_θ points within the locus represent an elastic state.

Consider first the representation of an unwrapped (all-metal) cylinder on this stress field. Hoop stress σ_θ is twice longitudinal stress σ_l throughout the total pressure range up to burst. Therefore the σ_l/σ_θ stress ratio plots as a straight line of gradient $\frac{1}{2}$ from the zero stress origin 0 to intersect the yield locus at point 1 where plastic deformation commences and continues at the same fixed stress ratio. Showing the yield locus as a single line is representative of a non-strain-hardening cylinder, or initial yielding of a strain-hardening cylinder. In the former case the cylinder would reach instability and burst at a pressure corresponding to point 1. In the latter case the yield locus would be represented by a band or zone, notionally bounded by the indicated dotted locus, through which the stress ratio line continues to the point of instability 1′

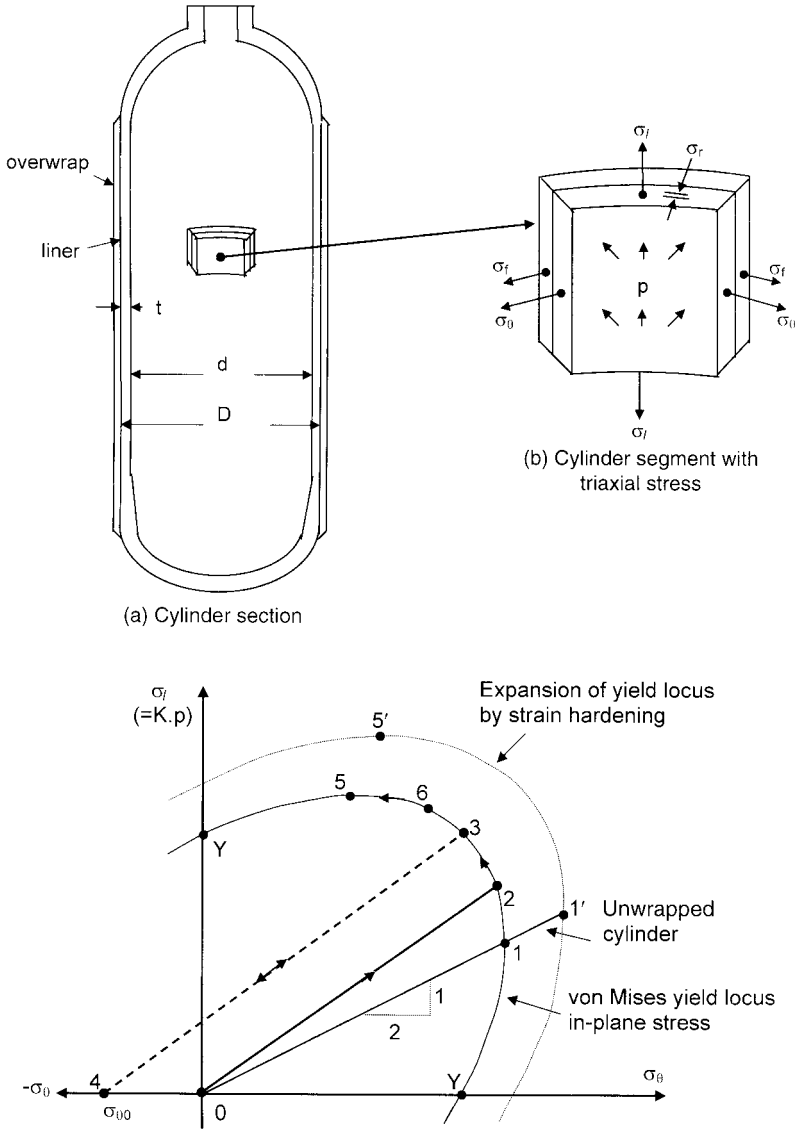

Fig. 1.1 Hoop-wrapped cylinder under internal pressure using plane stress analogy for visualizing liner yielding process

where σ_1, σ_0 and internal pressure p would all exceed those at point 1. Internal pressure at any stage along line 0–1 is found by putting point values of either σ_1 or σ_0 in the appropriate stress–pressure formula.

Consider now the hoop-wrapped cylinder in a manufactured state prior to autofrettage, i.e. with both principal stresses zeroed on origin 0. It is noteworthy that there is direct proportionality between longitudinal stress σ_1 and pressure p at all pressures up to burst, because fibre reinforcement applies in the hoop direction only. The effect of the wrap is to stiffen the liner against hoop expansion, and therefore during the initial pressurization for any value of σ_1 (i.e. of p), σ_0 will be less than that for the unwrapped cylinder. In other words, in the elastic phase the gradient of the stress ratio line will be greater for the wrapped cylinder, intersecting the yield locus at point 2 where plastic deformation commences. However, unlike the non-strain-hardening unwrapped cylinder, the reinforcement will prevent imminent hoop bursting of the liner, and pressurization will continue, leading to a situation of rising pressure and, therefore, rising longitudinal stress, together with plastic deformation. Such a state can only be reconciled by an anticlockwise rotation of the stress point σ_1, σ_0 along the yield locus, say to some point 3, during which interval hoop stress is *reducing*. If the cylinder is now depressurized, liner elastic recovery will take place from point 3 along a line parallel to line 0–2, resulting in a compressive hoop stress $\sigma_{\theta 0}$ at zero pressure as depicted by point 4. The load/unload cycle represented by $0 \rightarrow 2 \rightarrow 3 \rightarrow 4$ is recognized as autofrettage (this is discussed later in this section). Re-pressurization from point 4 causes stress increase along line $4 \rightarrow 3$ with yield reoccurring at point 3. Further pressurization results in continuance of the anticlockwise stress path along the

yield locus until one of two possible events occur as follows:

If the amount of fibre overwrap is excessive, travel along the locus will proceed to point 5, which represents maximum sustainable longitudinal stress $\sigma_{l\max}$ for a non-strain-hardening liner. Since σ_l is directly linked to internal pressure p, this point on the locus also represents maximum sustainable pressure $p_{\max}$ for the composite cylinder, and the cylinder will thus burst in a longitudinal mode. This same general conclusion is reached for a 'normal' strain-hardening liner, because the effect of plastic strain in increasing yield strength will be progressive from initial yielding at point 2, and therefore the $\sigma_{l\max}$ point (say 5′) approached asymptotically. The only difference will be an increased $p_{\max}$ resulting from expansion of the von Mises envelope.

If, on the other hand, the amount of fibre overwrap is sufficiently less than in the above case, pressurization above point 3, coupled with the already noted decrease in liner hoop stress contribution, will bring the fibre to its maximum tensile strength T_f and bursting of the cylinder will thus occur by hoop mode at some point 6 where $\sigma_l < \sigma_{l\max}$ and $p < p_{\max}$.

It follows from the two preceding studies that there is in theory a critical amount of fibre overwrap for any given liner that will cause bursting on a precise boundary separating hoop and longitudinal burst modes. Since the longitudinal burst mode is generally held unacceptable on safety grounds, definition of this critical changeover point in terms of the design variables is of fundamental importance, and accordingly receives considerable attention in the following development of the design theory.

However, by way of caution, it is important to note that the above theoretical conclusions are drawn purely on *stress* considerations of liner and fibre in the liner's plastic deformation phase. For both critical burst at p_{max} and hoop mode burst at $p < p_{max}$ there is the underlying implicit assumption that maximum fibre strain *is* developed in the process before unstable plastic strain develops in, and causes failure of, the liner. Clearly this situation cannot be generally true for all possible combinations of liner/fibre materials, because, for example, a high-strength fibre of elastic modulus significantly lower than that of the liner could have fracture strain greater than the instability strain of the liner, and then the theory would not apply. It is therefore important to check and confirm that the latter condition does not arise before applying this theory, although it is known that with commonly used liner/fibre material combinations the theoretical assumption is valid.

Figure 1.2 illustrates the three burst conditions described above, including representation of fibre stress. Figure 1.2a depicts a typical acceptable hoop burst where maximum fibre stress T_f is attained at a pressure corresponding to $\sigma_l < \sigma_{l\,max}$. Figure 1.2b depicts an unacceptable longitudinal burst where maximum longitudinal stress $\sigma_{l\,max}$ and maximum pressure p_{max} have been reached before maximum fibre stress due to excessive fibre. Figure 1.2c illustrates the important theoretical boundary condition where maximum liner longitudinal stress (and pressure) are reached simultaneously with development of maximum fibre stress.

Figure 1.3 shows the autofrettage process superimposed on the plane stress field, amplifying the previously introduced insight. Both liner and fibre loading/unloading

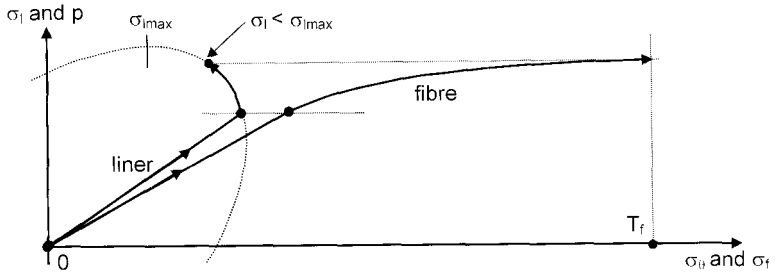

(a) Acceptable hoop burst mode initiated by fibre failure, $a_f < a_{fc}$

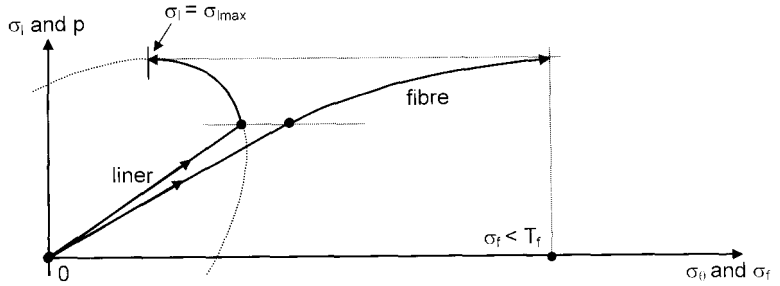

(b) Unacceptable longitudinal burst mode due to excessive fibre overwrap, $a_f > a_{fc}$

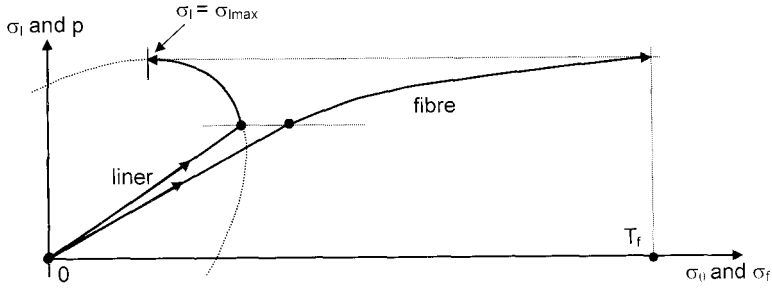

(c) The critical condition – longitudinal liner burst simultaneous with fibre failure, $a_f = a_{fc}$

Fig. 1.2 Plane stress analogy of burst modes for hoop-wrapped cylinders

characteristics are linear when the liner is in the elastic range. However during the liner's plastic deformation phase between initial yield and the autofrettage

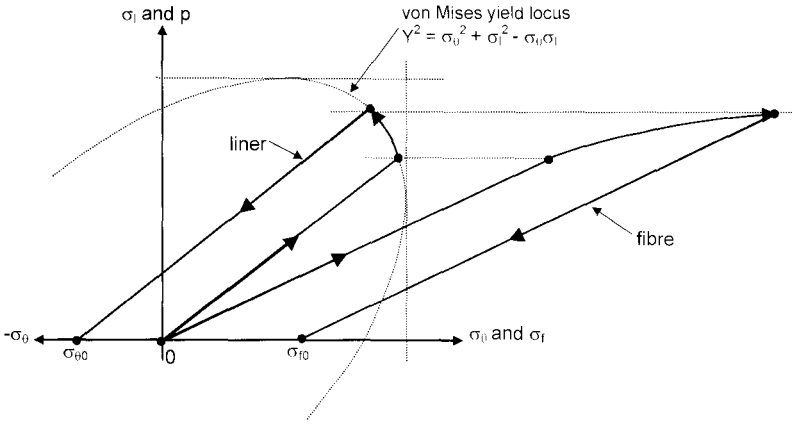

Fig. 1.3 Plane stress analogy of the autofrettage process

conditioning point, both liner and fibre exhibit non-linear stress versus pressure trends, even though the fibre remains linear elastic throughout; this is because the fibre is providing increasing proportional contribution to pressure load sharing as liner hoop stress reduces around the von Mises locus. A noteworthy feature of the autofrettage process, readily appreciated from Fig. 1.3, is that after re-pressurization to yield at the conditioning point, further pressurization causes resumption of plastic straining of the liner and elastic straining of the fibre just as though autofrettage had never taken place. It follows that autofrettage has no effect on subsequent cylinder bursting.

1.3 Prediction of the critical burst mode boundary cylinder design

The simplest approach is to assume a plane stress condition for the liner, as per the visualization in Section

1.2, but such an assumption is justified only if the radial through-wall stress is negligible compared with hoop and longitudinal stresses. It is shown in Section 1.3.2 that mean radial stress lies (numerically) between $p/2$ and p. Therefore the assumption will be least in error when internal pressure is small compared with yield stress. Given that service pressures are set by use considerations, this implies least error with higher yield stress liners. A typical alloy steel liner would have yield stress of around 800 MPa, and a composite cylinder based on such a liner would, for a service pressure of 200 bar, have a burst pressure of at least 500 bar. Therefore the internal pressure/yield stress ratio at burst would be of the order 50/800 or $\approx$6 percent, an amount which could not be taken as negligible. If a Series 6 aluminium alloy liner (as frequently used in hoop-wrapped composites) is considered with typical yield stress of 300 MPa at the same above pressures, the ratio becomes 50/300 or $\approx$17 percent, a significant amount, especially as 200 bar is by no means a high service pressure by modern standards. The effect of radial compressive stress in the von Mises criterion is to reduce values of hoop and longitudinal stress at which yielding occurs, in other words effectively to weaken the liner. Therefore, to ignore a significant radial stress is to overestimate cylinder performance – an untenable design position, and although the error would be graver in some cases than others, as indicated above, a comprehensive theory should accommodate all potential cases.

Following from the above, the need to include radial stress in critical burst theory was recognized at an early stage. However, it remained convenient in developing the theory to start simple and subsequently build in refinement. In the interests of presentation the same procedure is repeated below.

1.3.1 Burst boundary evaluation for the plane stress condition

Ignoring radial stress, the von Mises yield criterion appears as in Section 1.2

$$Y^2 = \sigma_\theta^2 + \sigma_l^2 - \sigma_\theta \cdot \sigma_l$$

Differentiating

$$2Y \cdot dY = 2(\sigma_\theta \cdot d\sigma_\theta + \sigma_l \cdot d\sigma_l) - \sigma_l \cdot d\sigma_\theta - \sigma_\theta \cdot d\sigma_l$$

At maximum pressure $d\sigma_l = 0$, and since yield stress is considered constant $dY = 0$. It follows that at maximum pressure $\sigma_\theta = \sigma_l/2$.

Substituting for σ_θ in von Mises, gives for the critical burst condition

$$\sigma_l = (2/\sqrt{3})Y \qquad \sigma_\theta = (1/\sqrt{3})Y$$

(The stress ratios $\sigma_l, \sigma_\theta = \sigma_l/2, \sigma_r = 0$ represent plane strain with $\varepsilon_\theta = 0$.)

Since σ_l is given generally by $pd^2/(D^2 - d^2)$, the critical burst pressure is

$$p_{bc} = \frac{2Y(D^2 - d^2)}{\sqrt{3}d^2}$$

and total fibre cross-sectional area a_{fc} at critical burst p_{bc} is given by the hoop equilibrium equation, putting $p = p_{bc}, \sigma_f = T_f$, and $\sigma_\theta = (1/\sqrt{3})Y$, thus

$$a_{fc} = \frac{p_{bc} \cdot a_{c\theta} - \frac{1}{\sqrt{3}} Y \cdot a_\theta}{T_f}$$

The above analysis, though overly simplified for practical application, demonstrates how an understanding of the plastic behaviour of the liner leads directly to a prediction of the critical burst pressure. According to the analysis, a

liner of proportions D, d, t with a non-strain-hardening yield stress Y, will have a critical burst pressure p_{bc}, and the amount of fibre of strength T_f to just cause fibre failure at this pressure has cross-sectional area $a_{fc}/2$ on each side.

Radial wall stress is introduced to the theory in the next stage of development.

1.3.2 A first approximation to burst boundary with a triaxial stress state

For triaxial liner stress the von Mises yield criterion is

$$2Y^2 = (\sigma_\theta - \sigma_l)^2 + (\sigma_l - \sigma_r)^2 + (\sigma_r - \sigma_\theta)^2$$

The same analytical procedure is followed as in Section 1.3.1 except that it is assumed that σ_r is a function of internal pressure p only, and therefore at critical liner burst pressure p_{bc} not only are dY and $d\sigma_l$ equal to zero, but also $d\sigma_r$ is zero. This leads to the result that at pressure p_{bc},

$$\sigma_\theta = \tfrac{1}{2}(\sigma_l + \sigma_r).$$

Substituting this value into the yield criterion gives at p_{bc}

$$\sigma_{l\max} = \left(\frac{2}{\sqrt{3}}\right) Y + \sigma_r$$

and corresponding

$$\sigma_\theta = \left(\frac{1}{\sqrt{3}}\right) Y + \sigma_r$$

Since σ_r is compressive and, therefore, according to convention negative, $\sigma_{l\max}$ and connected critical burst pressure p_{bc} will be less than given by the plane stress theory of Section 1.3.1.

The problem with applying this version of the theory is that mean radial stress σ_r is unknown and can only be surmised to lie somewhere between $\sigma_r = -p/2$, i.e. that for an unwrapped cylinder, and $\sigma_r = -p$, as would result from total hoop reinforcement. The next, final, stage of critical burst theory development includes a more fundamental treatment of radial stress.

1.3.3 Rigorous theory of the critical burst boundary condition

1.3.3.1 Radial stress

A complete expression for mean radial liner stress is provided by considering the forces acting on a half-hoop section of the composite cylinder, analysing equilibrium of the two components together and separately. Figure 1.4a shows the combined cross-section where hoop load generated by internal pressure p acting on cross-section $a_{c\theta}$ is reacted by the combined force of fibre stress σ_f acting on area a_f and liner hoop stress σ_θ acting on area a_θ. Thus for the composite cylinder, hoop equilibrium is given at all pressures by

$$p \cdot a_{c\theta} = \sigma_f \cdot a_f + \sigma_\theta \cdot a_\theta$$

Figure 1.4b shows equilibrium of the fibre overwrap as a separate element, where pressure p_i developed at the liner/fibre interface area a_{ci} is reacted by fibre stress σ_f acting on area a_f. Thus for equilibrium

$$p_i \cdot a_{ci} = \sigma_f \cdot a_f$$

Figure 1.4c shows equilibrium of the liner as a separate element with *internal* pressure p acting on the effective internal area $a_{c\theta}$ and *external* pressure p_i arising from fibre constraint acting on the effective interface area a_{ci}.

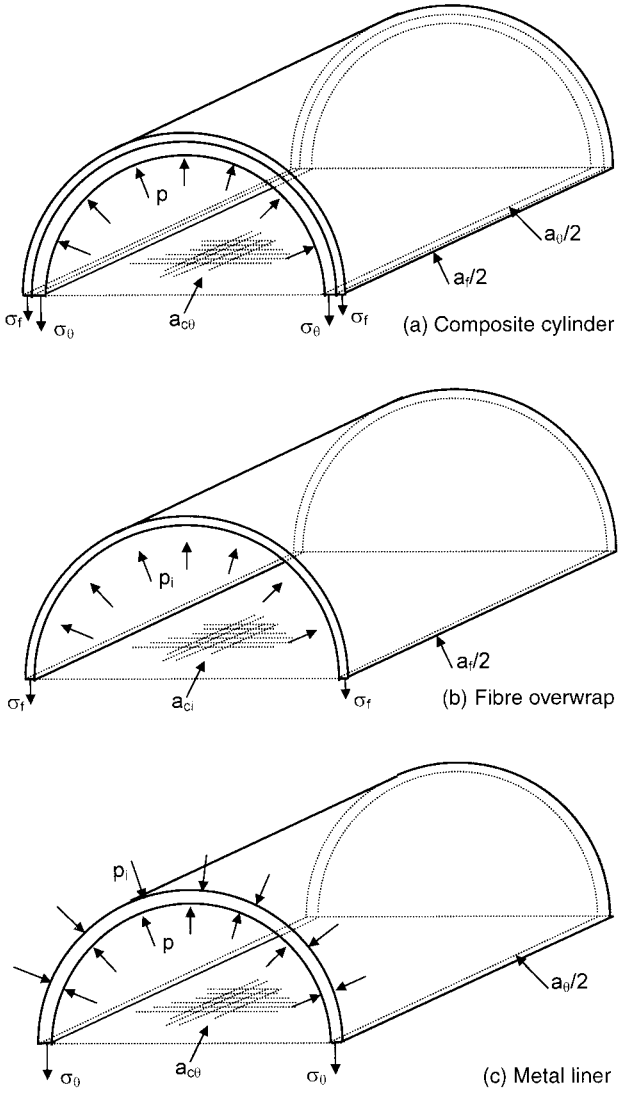

Fig. 1.4 Hoop equilibrium of cylinder and component parts

For equilibrium

$$p \cdot a_{c\theta} - p_i \cdot a_{ci} = \sigma_\theta \cdot a_\theta$$

and thus

$$p_i = (p \cdot a_{c\theta} - \sigma_\theta \cdot a_\theta)/a_{ci}$$

Now radial stress at the liner inner surface is $-p$, and radial stress at the interface is $-p_i$. Therefore mean radial through-wall stress $\sigma_r = -(p + p_i)/2$. Substituting for p_i and rearranging gives

$$\sigma_r = \tfrac{1}{2}(a_\theta/a_i) \cdot \sigma_\theta - \tfrac{1}{2}(1 + a_{c\theta}/a_{ci}) \cdot p$$

where

$$a_\theta = 2t/\text{unit length}$$
$$a_{c\theta} = d/\text{unit length}$$
$$a_{ci} = D/\text{unit length}$$

The term $\frac{1}{2}(a_\theta/a_{ci})$ therefore reduces to t/D, and the term $\frac{1}{2}(1 + a_{c\theta}/a_{ci})$ to $(1 - t/D)$.

Letting design constant $t/D = A$, the above expression for σ_r reduces to

$$\sigma_r = A \cdot \sigma_\theta - (1 - A) \cdot p \qquad (1.1)$$

Thus mean radial liner stress is seen to be a function of both internal pressure and hoop stress, which theoretically invalidates the simplifying assumption made in the earlier treatment of Section 1.3.2.

1.3.3.2 Development of the theory

Although σ_r from equation (1.1) could be used in expressions for $\sigma_{l\max}$ and σ_θ derived in Section 1.3.2 to provide a result for critical burst pressure p_{bc}, this approach is not strictly correct because σ_r should be

treated as variable in both p and σ_θ in the derivation, as shown below.

The triaxial von Mises yield criterion introduced in Section 1.3.2 can be expanded to

$$Y^2 = \sigma_\theta^2 + \sigma_l^2 + \sigma_r^2 - \sigma_\theta \cdot \sigma_l - \sigma_l \cdot \sigma_r - \sigma_r \cdot \sigma_\theta \tag{1.2}$$

Differentiating, and noting that $dY = 0$ for constant current yield stress, and $d\sigma_l = 0$ at maximum pressure, the critical boundary condition is expressed by

$$0 = d\sigma_\theta(2\sigma_\theta - \sigma_l - \sigma_r) + d\sigma_r(2\sigma_r - \sigma_l - \sigma_\theta) \tag{1.3}$$

A link between $d\sigma_\theta$ and $d\sigma_r$ is given by differentiating equation (1.1), and putting $dp = 0$ at critical burst

$$d\sigma_r = A \cdot d\sigma_\theta \tag{1.4}$$

Combining equations (1.3) and (1.4) gives a relationship between the principal stresses at the critical boundary, thus

$$(2 - A)\sigma_\theta = (1 - A)\sigma_l - (2A - 1)\sigma_r \tag{1.5}$$

Equations (1.1), (1.2), and (1.5) are three relationships between the three unknown principal stresses σ_θ, σ_l, and σ_r at the critical burst boundary, and hence in combination they provide the means of defining the pressure and associated stresses at that important condition. The method of derivation followed, which seems to offer least mathematical resistance, is to first substitute σ_θ from equation (1.5) into von Mises equation (1.2), providing a relationship between σ_l, σ_r, and Y. The structure of equation (1.2) makes the procedure cumbersome, but the outcome is an expression for critical longitudinal

stress, thus

$$\sigma_{l\max} = \frac{Y}{\sqrt{3}}\left[\frac{2-A}{\sqrt{(A^2-A+1)}}\right] + \sigma_r \tag{1.6}$$

Corresponding hoop stress at the critical boundary is obtained by substituting σ_l from equation (1.6) in equation (1.5)

$$\sigma_\theta = \frac{Y}{\sqrt{3}}\left[\frac{1+A}{\sqrt{(A^2-A+1)}}\right] + \sigma_r \tag{1.7}$$

The route is now clear for establishing critical boundary burst pressure p_{bc}, because combining equation (1.7) with equation (1.1) to eliminate σ_θ gives an expression for σ_r in terms of p_{bc}, which is then used in equation (1.6), writing $\sigma_{l\max}$ in terms of p_{bc} and area parameter K, as follows:

From equations (1.7) and (1.1)

$$\sigma_r = \frac{Y}{\sqrt{3}}\left[\frac{A(1+A)}{(1-A)\sqrt{(A^2-A+1)}}\right] - p_{bc} \tag{1.8}$$

Substituting for σ_r in equation (1.6), putting $\sigma_{l\max} = K \cdot p_{bc}$, gives

$$p_{bc} = \frac{2Y}{\sqrt{3}}\left[\frac{\sqrt{(A^2-A+1)}}{(K+1)(1-A)}\right]$$

and noting that $(K+1) = 1/[4A(1-A)]$

$$p_{bc} = \frac{8Y}{\sqrt{3}} \cdot A\sqrt{(A^2-A+1)} \tag{1.9}$$

Having derived critical burst pressure p_{bc}, closed-form expressions for σ_r from equation (1.8), σ_θ from equation (1.7), and σ_l from equation (1.6) all follow. These are included in Annex 1 in two forms. The first form gives σ_θ, σ_l, and σ_r in terms of the basic parameters A and Y.

The second form, which provides simpler expressions, incorporates additionally p_{bc}, as the latter will usually be evaluated before solving for principal stresses. However, it is noted that probably the easiest way to establish the burst boundary condition is to ignore these closed expressions and instead apply the theory in a stepwise manner, first deducing p_{bc} from equation (1.9), then deducing $\sigma_{l\max}$ directly from $K \cdot p_{bc}$, then deducing σ_r from equation (1.6), and then deducing σ_θ from equation (1.7). This and other aspects of applying the theory to cylinder design are covered in Part 2.

Although in the preceding development critical boundary pressure p_{bc} is derived in terms of liner wall thickness/diameter ratio A, in practice the cylinder designer is more likely to be faced with evaluating A for a prescribed value of p_{bc}, and then equation (1.9) must be solved instead for A, which is less straightforward. A simple numerical approach is generally best, noting to start with that since A is small the term $\sqrt{(A^2 - A + 1)}$ is just less than unity, and therefore a first approximation to A is given by $A_0 = \sqrt{3} \cdot p_{bc}/(8Y)$. By substituting this value as A in $A\sqrt{(A^2 - A + 1)}$ and comparing the result with $\sqrt{3} \cdot p_{bc}/(8Y)$, A is increased by the difference, in steps, until $A\sqrt{(A^2 - A + 1)} = \sqrt{3} \cdot p_{bc}/(8Y)$. [An alternative less precise approach is to note that for small A, the term $\sqrt{(A^2 - A + 1)}$ approximates $\sqrt{(1 - A)}$, which can be further approximated from binomial expansion by $(1 - A/2)$. Thus replacing $A\sqrt{(A^2 - A + 1)}$ by $A(1 - A/2)$ reduces equation (1.9) to a quadratic in A.]

Table 1.1 compares critical boundary burst pressures from the rigorous theory with those from the simple 'plane stress' theory of Section 1.3.1. It is seen that over a t/D range from 0 to 0.060 (which encompasses most hoop-wrapped cylinders) the error of the simple theory ranges from 0 to almost 25 percent overestimate. Typical alloy

Table 1.1 Comparison of critical burst pressure from plane stress and triaxial stress theories and principal stress ratios from triaxial theory

		Triaxial stress theory			
Thickness/ diameter ratio $A = t/D$	*Critical burst pressure ratio: plane stress theory/triaxial stress theory*	σ_0/Y	σ_l/Y	σ_r/Y	σ_0/σ_l
0	1.000	0.577	1.155	0	0.500
0.010	1.036	0.546	1.115	−0.040	0.490
0.020	1.074	0.515	1.075	−0.079	0.479
0.030	1.114	0.486	1.037	−0.118	0.469
0.040	1.156	0.457	0.999	−0.156	0.457
0.050	1.202	0.428	0.961	−0.193	0.445
0.060	1.245	0.401	0.924	−0.229	0.434

$$\text{Plane stress } p_{bc} = \frac{2Y}{\sqrt{3K}} = \frac{2Y}{\sqrt{3}}\left[\frac{4A(1-A)}{1-4A(1-A)}\right]$$

$$\text{Ratio: } \frac{\text{Plane stress } p_{bc}}{\text{Triaxial stress } p_{bc}} = \left[\frac{1-A}{\{1-4A(1-A)\}\sqrt{(1-A+A^2)}}\right]$$

steel liners would have t/D ranging approximately from 0.015 to 0.022, depending on service pressure, with associated 5–8 percent overestimate, typical 6000 Series aluminium alloy liners would have t/D ranging around 0.040 to 0.060, with an associated 15–24 percent overestimate. These data clearly justify the need for the rigorous triaxial stress theory.

Table 1.1 also shows how principal stresses σ_0, σ_l, and σ_r associated with critical burst pressure p_{bc} vary with t/D according to the rigorous theory for any given current yield stress Y. Importantly, it is noted that liner hoop stress

σ_θ at critical burst is generally less than one-half of longitudinal stress σ_l, with implications for fibre reinforcement discussed later.

Knowledge of liner hoop stress σ_θ at critical burst pressure p_{bc}, as provided by equation (1.7), enables calculation of critical fibre area a_{fc} required to induce boundary failure, thus

$$a_{fc} = \frac{p_{bc} \cdot a_{c\theta} - \sigma_\theta \cdot a_\theta}{T_f} \tag{1.10}$$

If $a_f < a_{fc}$, bursting will occur by hoop mode, and if $a_f > a_{fc}$, bursting will be by longitudinal (separation) mode. Special note is made that σ_θ in equation (1.10) is a *particular* value of liner hoop stress given uniquely by equation (1.7).

Note
Implicit in equation (1.10) is the assumption that full fibre strain to fracture is developed before plastic instability strain in the liner occurs. Unless this condition is already known to be true for the liner/fibre materials of the design, it should be checked using the procedure given in Section 1.9.

1.3.4 Effect of strain-hardening on liner yield strength at the critical boundary

Throughout Section 1.3, and particularly in Section 1.3.3, equations (1.2) to (1.9), Y is the liner's current yield stress at the point of critical burst, and therefore is greater than the initial yield stress of the liner as manufactured because of strain-hardening undergone in the plastic deformation phase. The need to ascribe a realistic value of Y is clear since it directly affects the numerical value of calculated stresses and pressures, not only at critical burst but also in other aspects of cylinder design theory described below.

General analysis for evaluating current yield stress at burst with strain-hardening is included in Section 1.9.

1.4 General hoop burst theory

From equation (1.10) it follows that for a liner of area a_θ, hoop bursting will occur for all values of fibre area a_f less than a_{fc}. This range is notionally represented by points 1 to 5 in Fig. 1.1c, where point 1 is the unwrapped cylinder with $a_f = 0$, and advance around the von Mises locus represents increasing fibre area and corresponding increasing burst pressure, from that of the unwrapped liner p_{bl} to the critical burst p_{bc}. (Theory for burst pressure of the unwrapped liner is developed in Annex 2.)

For any given pressure p_b, where $p_{bl} < p_b < p_{bc}$, and liner wall area a_θ, longitudinal stress is known, being given by $\sigma_l = K \cdot p_b$, hoop stress σ_θ is unknown, and radial stress σ_r, given by equation (1.1), can be written in terms of σ_θ and p_b. Thus the only unknown in the von Mises yield criterion is σ_θ. Substituting $\sigma_l = K \cdot p_b$, $\sigma_r = A \cdot \sigma_\theta - (1 - A)p_b$ in equation (1.2) leads to the quadratic

$$\sigma_\theta^2 - m \cdot \sigma_\theta + n = 0$$

and hence

$$\sigma_\theta = \frac{m}{2}\left[1 + \sqrt{(1 - 4n/m^2)}\right] \tag{1.11}$$

where

$$m = p_b\left[\frac{K(1 + A) - (1 - A)(1 - 2A)}{1 - A + A^2}\right]$$

and

$$n = \frac{p_b^2\left[K^2 + (1-A)^2 + (1-A)K\right] - Y^2}{1 - A + A^2}$$

In equation (1.11) the positive root only has been taken, since this represents the stress condition of interest on the von Mises yield locus. Two noteworthy special cases of equation (1.11) arise. Firstly, when the term $4n/m^2 = 1, \sigma_\theta = m/2$ irrespective of the root sign, i.e. there is a single value for σ_θ, and this in fact corresponds to the critical burst condition, representing the limit of the general hoop burst theory. No real values exist for σ_θ when $4n/m^2 > 1$. Secondly, when $n = 0$, equation (1.11) gives $\sigma_\theta = m$. However, the corresponding negative root of equation (1.11) gives $\sigma_\theta = 0$. Therefore the particular value of $\sigma_\theta = m$ given by equation (1.11) when $n = 0$, should be given no greater significance than this as far as prediction of the theory is concerned.

Knowing hoop stress σ_θ at p_b from equation (1.11), consideration of hoop equilibrium provides the fibre area a_{fb} necessary to cause hoop burst at p_b, i.e.

$$a_{fb} = \frac{p_b \cdot a_{c\theta} - \sigma_\theta \cdot a_\theta}{T_f} \tag{1.12}$$

Radial stress σ_r follows from equation (1.1) and therefore all three principal stresses in the liner at p_b are known.

Note 1

Implicit in equation (1.12) and in this theory in general, is the assumption that full fibre strain to fracture is developed before plastic instability strain in the liner occurs. Unless this condition is already known to be true for the liner/fibre materials of the design, it should be checked using the procedure in Section 1.9.

Note 2

Although the stress theory developed in this section is concerned with the hoop burst situation, the underlying concepts are not limited to this situation, and can be applied in the broader context of cylinder behaviour when the liner is in a plastic state. This follows because providing that the cylinder's burst pressure p_b is less than the critical burst pressure p_{bc}, bursting under the postulated conditions can only result from fibre failure, causing in turn, pressure overload of the liner. At pressures less than p_{bc}, providing that the fibre remains intact, the liner will be in a stable plastic state with principal stresses satisfying the von Mises yield criterion. Thus equation (1.11) may be used generally to derive hoop stress σ_0 at *any* pressure p, where $p_{y0} < p < p_b$. Likewise, equation (1.12) may be used to obtain the fibre area a_f versus fibre stress σ_f relationship at that pressure and hoop stress, within the confines of $\sigma_f < T_f$, $a_f < a_{fc}$. A particular example of such an application is the case of autofrettage.

1.4.1 Effect of strain-hardening on hoop burst pressure

The importance of using a realistic value of current yield stress Y in equation (1.11) is self-evident, and Y depends on the amount of strain-hardening from initial yielding to failure. Over the range of failure represented by $p_{bl} < p_b < p_{bc}$ the nature of liner straining changes significantly. Bursting of the unwrapped and lightly wrapped liner is mainly characterized by hoop straining, longitudinal strain being low because of the near plane strain condition. However bursting at critical pressure p_{bc} involves a varying range of straining modes culminating at the point of bursting with high-longitudinal and low-hoop strain increments. While it is clear that, in general, hoop

bursting involves hoop strain equal to maximum fibre tensile strain (a quantity readily established), the accompanying longitudinal strain will increase progressively around the yield locus as p_b increases towards p_{bc}. Hence it is to be expected that *equivalent* strain and current yield stress Y will increase commensurately. With the relatively high yield/tensile materials used for gas cylinder liners, the potential for error in this area is reduced but is still significant. Section 1.9 provides quantitative analysis on the subject.

1.5 Design burst optimization

There are two elements to be considered: firstly deciding a cylinder *design* burst pressure in relation to the *critical* burst pressure p_{bc}, and secondly establishing the fibre reinforcement necessary to cause bursting at the decided *design* burst pressure. Since the *design* burst mode will always be hoop, *design* burst is a particular case of and fully defined by the general hoop burst theory of Section 1.4.

1.5.1 Cylinder design burst pressure

The starting point will often be a minimum burst pressure *required* by specification and/or regulation, typically in the form of an arbitrary multiple of the service or hydrostatic test pressure. Such a requirement, when it exists, sets an absolute minimum burst pressure for the cylinder. Let this pressure be p_{br}. Because theory cannot provide total accuracy, and manufacture cannot provide total process control, *design* burst pressure would normally be set with a margin above p_{br}, otherwise there is a risk that the design will not always achieve p_{br} on test. Thus, if *design* burst

pressure is p_{bd}, then $p_{bd} > p_{br}$. Finally, to ensure that the cylinder bursts in hoop mode there is a condition that p_{bd} is less than *critical* burst pressure p_{bc}. Hence the general condition $p_{br} < p_{bd} < p_{bc}$ can be written, with separating margins dependent on design/manufacturing confidence. For equal margin between *required* and *critical* conditions $p_{bd} = (p_{br} + p_{bc})/2$.

1.5.2 Design burst theory

Having decided p_{bd} and p_{bc} relative to minimum burst p_{br}, equation (1.9) is applied to establish the liner wall thickness necessary to achieve p_{bc} at the given diameter. This sets the $t/D(= A)$ value, ensuring longitudinal bursting will not occur at p_{bd}.

The general theory developed in Section 1.4 is applied, substituting p_{bd} for p_b, thus

$$\sigma_\theta = \frac{m}{2}\left[1 + \sqrt{(1 - 4n/m^2)}\right] \tag{1.11a}$$

where

$$m = p_{bd}\left[\frac{K(1 + A) - (1 - A)(1 - 2A)}{1 - A + A^2}\right]$$

and

$$n = \frac{p_{bd}^2\left[K^2 + (1 - A)^2 + (1 - A)K\right] - Y^2}{1 - A + A^2}$$

Knowing hoop stress σ_θ at p_{bd} from equation (1.11a), consideration of hoop equilibrium provides the fibre area a_{fd} necessary to cause hoop burst at p_{bd}, i.e.

$$a_{fd} = \frac{p_{bd} \cdot a_{c\theta} - \sigma_\theta \cdot a_\theta}{T_f} \tag{1.12a}$$

Radial stress σ_r follows from equation (1.1) and therefore all three principal stresses in the liner at p_{bd} are known.

It is observed that the proportional increase in fibre area from a_{fd} at *design* burst to a_{fc} at *critical* burst [equation (1.10)], significantly exceeds the corresponding proportional increase in burst pressure achieved from p_{bd} to p_{bc}, reflecting the decreasing contribution of the liner hoop stress to the hoop load, as can be appreciated from Fig. 1.2.

Note
Implicit in equation (1.12a) is the assumption that full fibre strain to fracture is developed before plastic instability strain in the liner occurs. Unless this condition is already known to be true for the liner/fibre materials of the design, it should be checked using the procedure in Section 1.9.

1.5.3 Effect of strain-hardening on yield strength at design burst

In practical terms the *design* burst pressure will usually be sufficiently close to the *critical* burst pressure to give plastic straining and current yield stress approaching that in the latter. Section 1.9 provides quantitative analysis.

1.6 Linear elastic stress theory

The cylinder will normally operate in the elastic state throughout its working life and elastic operating stress levels are important and must be quantified. However, it is noteworthy that the main elements of the cylinder design have already been set by preceding burst considerations based on plastic state analysis, namely: the *critical* burst theory of Section 1.3.3 provided liner wall thickness, and

the *design* burst theory of Section 1.5.2 provided fibre area. (These elements *could* subsequently be revised upwards if resulting elastic stresses are too high to achieve the required number of fatigue cycles.) Furthermore, as will later be seen, the distribution of elastic stress between liner and fibre, though defined by elastic safety factor requirements, is actually imparted by controlled plastic deformation of the liner.

In the interests of accuracy and compatibility of stress across the elastic/plastic interface, the general state of triaxial stress used in burst theory is retained for elastic analysis.

Manufacture and use of a hoop-wrapped cylinder involves two separate elastic stress states. The first concerns loading the cylinder from zero stress up to initial yield as part of the manufacturing autofrettage process. The second concerns the general state of stress during normal use after autofrettage. Both states are analysed in the following sub-sections.

The elastic stress state in liner and fibre at any given pressure can be derived by the application of two simultaneous conditions:

(a) equilibrium of hoop forces,
(b) equality of hoop strain increment in liner and fibre.

1.6.1 Elastic stress prior to autofrettage

Figure 1.5a shows liner hoop stress σ_0 versus pressure p. For any applied pressure $p(0 < p < p_{y0})$, consideration of hoop equilibrium gives

$$\sigma_f = \frac{p \cdot a_{c\theta} - \sigma_0 \cdot a_0}{a_f} \tag{1.13}$$

Since straining is from the zero stress/strain origin, equality of hoop strain provides a further relationship between fibre stress σ_f and liner hoop stress σ_θ

$$\sigma_f = \frac{E_f}{E_l}[\sigma_\theta - \nu(\sigma_l + \sigma_r)] \tag{1.14}$$

where $\sigma_l = K \cdot p$, and $\sigma_r = A \cdot \sigma_\theta - (1 - A) \cdot p$ from equation (1.1).

Substituting for σ_l and σ_r in equation (1.14), and equating with equation (1.13) leads to a general expression for liner hoop stress σ_θ in terms of p and cylinder constants

$$\sigma_\theta = p\left\{\frac{(a_{c\theta}/a_f) + (E_f/E_l)\nu(K - 1 + A)}{(E_f/E_l)(1 - \nu A) + (a_\theta/a_f)}\right\}$$

The bracket { } is a coefficient defining the gradient of the $\sigma_\theta \sim p$ line. Let this {coefficient} be Z, then

$$\sigma_\theta = Z \cdot p \tag{1.15}$$

Longitudinal stress $\sigma_l = K \cdot p$ is known, and σ_r is available by combining equations (1.15) and (1.1). Therefore all liner principal stresses are known in terms of pressure p, and corresponding fibre stress σ_f is obtained by combining equations (1.15) and (1.13).

1.6.2 Elastic state after autofrettage

Figure 1.5b shows the post-autofrettage elastic recovery line 3 → 4 of Fig. 1.1c added to Fig. 1.5a. All subsequent elastic relationship between hoop stress and pressure, loading and unloading, will be along this line. At zero pressure there will be a residual compressive stress in the liner $\sigma_{\theta 0}$, and a corresponding residual tensile stress in the

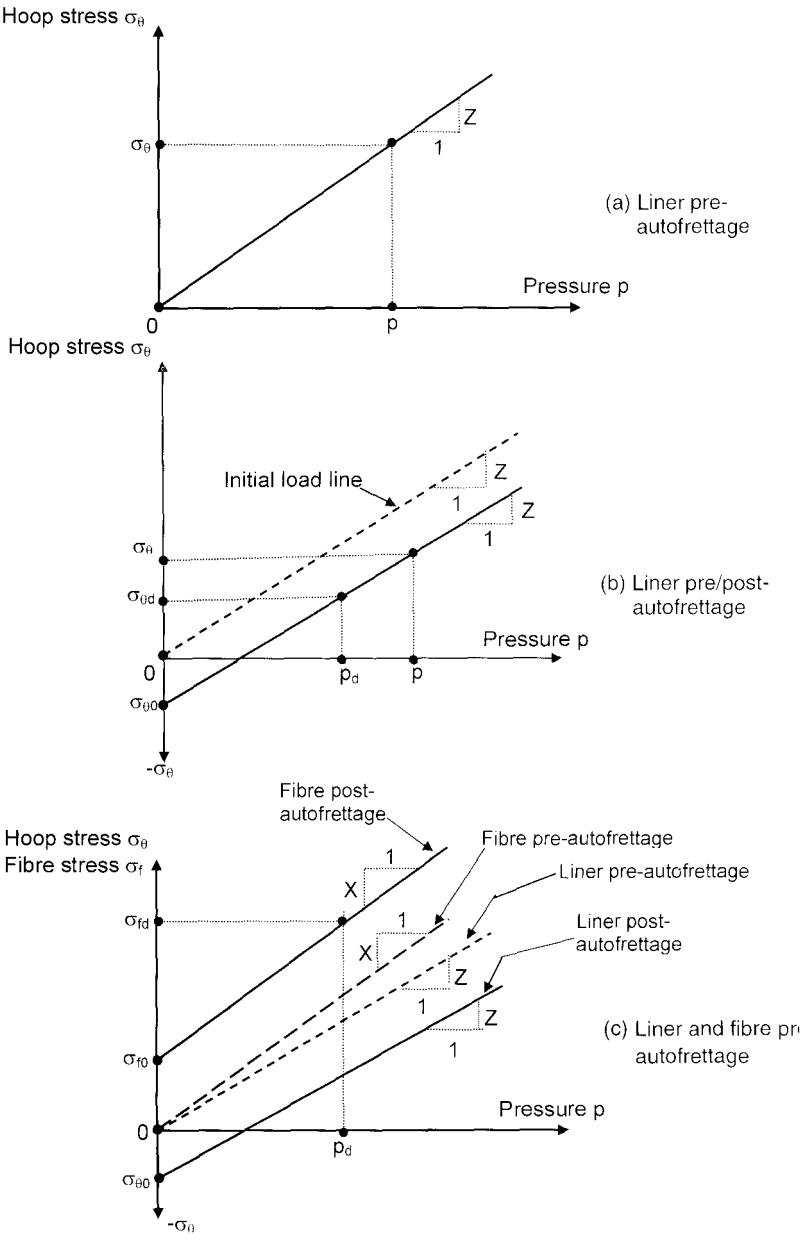

Fig. 1.5 Hoop and fibre stress versus pressure in the elastic range

fibre σ_{f0}. Because the stress line does not pass through the σ_θ–p origin, it is necessary to develop the σ_0 versus p relationship in terms of a 'design pressure' p_d at which 'design stresses' $\sigma_{\theta d}, \sigma_{ld}, \sigma_{rd}$, and σ_{fd} are nominated. The 'design pressure' could be any pressure between 0 and p_{y0} for the purpose of this theory, although it will be shown later that the imposition of a fibre stress ratio (FSR) as required in composite cylinder standards, effectively fixes p_d and all associated design stresses. The development of the σ_θ–p relationship proceeds as follows.

For any applied pressure p, consideration of hoop equilibrium again results in equation (1.13). Applying the strain equality condition over the strain increment corresponding to pressure $p_d \rightarrow p$ results in

$$\sigma_f = \frac{E_f}{E_l}[(\sigma_\theta - \nu\langle\sigma_l + \sigma_r\rangle) - (\sigma_{\theta d} - \nu\langle\sigma_{ld} + \sigma_{rd}\rangle)] + \sigma_{fd}$$

and substituting $\sigma_l = K \cdot p$, $\sigma_r = A \cdot \sigma_\theta - (1 - A)p$

$$\sigma_f = \frac{E_f}{E_l}\Big[\big(\sigma_0\langle 1 - \nu A\rangle - \nu p\langle K - 1 + A\rangle\big)$$

$$-\big(\sigma_{\theta d}\langle 1 - \nu A\rangle - \nu p_d\langle K - 1 + A\rangle\big)\Big] + \sigma_{fd} \qquad (1.16)$$

Equating equations (1.13) and (1.16) to eliminate σ_f, leads to a general expression for hoop stress σ_θ in terms of pressure p, the cylinder constants, and the designated design pressure/stresses

$$\sigma_\theta = p\left\{\frac{(a_{c\theta}/a_f) + (E_f/E_l)\nu(K - 1 + A)}{(E_f/E_l)(1 - \nu A) + (a_\theta/a_f)}\right\}$$

$$+\left[\frac{(E_f/E_l)(\sigma_{\theta d}\langle 1 - \nu A\rangle - \nu p_d\langle K - 1 + A\rangle) - \sigma_{fd}}{(E_f/E_l)(1 - \nu A) + (a_\theta/a_f)}\right]$$

Although this expression appears at first sight unwieldy, there is a basic underlying simplicity. By comparison with the pre-autofrettage expression (1.15) it is clear that the coefficient of p in the { } bracket is in fact Z, proving that the gradient of the hoop stress–pressure line is unchanged by autofrettage. Furthermore, the term in the [ ] bracket is observed to be constant for any given design pressure for *all* values of variable pressure p. Thus, putting $p = 0$ reveals that bracket [ ] is in fact the value of liner pre-stress, i.e. [ ] $= \sigma_{\theta 0}$. The above general expression for hoop stress after autofrettage can therefore be written

$$\sigma_\theta = Z \cdot p + \sigma_{\theta 0} \tag{1.17}$$

where

$$Z = \left\{ \frac{(a_{c\theta}/a_f) + (E_f/E_l)\nu(K - 1 + A)}{(E_f/E_l)(1 - \nu A) + (a_0/a_f)} \right\}$$

and

$$\sigma_{\theta 0} = \left[\frac{(E_f/E_l)(\sigma_{\theta d}\langle 1 - \nu A\rangle - \nu p_d\langle K - 1 + A\rangle) - \sigma_{fd}}{(E_f/E_l)(1 - \nu A) + (a_0/a_f)} \right]$$

Fibre stress at p is given by substituting for σ_θ from equation (1.17) into equation (1.13), longitudinal and radial stresses being evaluated as previously. However, the following Section 1.6.3 indicates an alternative, simpler, route to solution by considering fibre stress first.

1.6.3 Design pressure and associated stresses

While Section 1.6.2 shows stress analysis approached via liner considerations, it has become the practice in writing contemporary 'performance-based' composite cylinder standards to define a maximum fibre stress, rather than a maximum liner stress, in the elastic use range, to ensure that

in the long term there is no sudden fibre fracture leading to catastrophic cylinder failure, due to sustained stress loading. Fortuitously this practice is readily incorporated in, and indeed simplifies, the present design theory as follows:

Substituting hoop stress σ_θ from equation (1.17) into equation (1.13) gives fibre stress σ_f in terms of pressure p

$$\sigma_f = p\left[\frac{a_{c\theta} - Z \cdot a_\theta}{a_f}\right] - \left[\frac{a_0}{a_f}\right]\sigma_{\theta 0}$$

Now the term $-[a_0/a_f]\sigma_{\theta 0}$ is seen to be the fibre pre-stress σ_{f0} when $p = 0$. The coefficient $[a_{c\theta} - Z \cdot a_\theta]/a_f$ is a constant, because its constituents are design constants. Let this be X. The general expression for fibre stress is therefore

$$\sigma_f = X \cdot p + \sigma_{f0} \tag{1.18}$$

Now fibre stress ratio (FSR) is defined as the ratio of the tensile strength of the wrapped fibre to the fibre stress at a stated design pressure. Thus for fibre tensile strength T_f, design pressure p_d, fibre stress at design pressure is $\sigma_{fd} = T_f/\text{FSR}$. Substituting these *particular* values of fibre stress and pressure in equation (1.18) gives the value of fibre pre-stress σ_{f0} directly, thus

$$\sigma_{f0} = \frac{T_f}{\text{FSR}} - X \cdot p_d \tag{1.19}$$

and it follows from equation (1.13) that corresponding liner pre-stress is

$$\sigma_{00} = -\left(\frac{a_f}{a_\theta}\right)\sigma_{f0} \tag{1.20}$$

With knowledge of pre-stresses σ_{00} and σ_{f0}, general equations (1.17) and (1.18) can readily be applied across the elastic range, providing the means of deducing a complete stress–pressure map for liner and fibre.

Figure 1.5c depicts the general stress–pressure relationships for liner hoop and fibre before and after autofrettage. The gradient of liner hoop stress is Z, and that for fibre stress is X, both being constants for the particular design. At any given pressure p, stress difference due to autofrettage is $-\sigma_{00}$ for the liner and $+\sigma_{f0}$ for the fibre. It is observed from Fig. 1.5c that the use of FSR to define maximum allowable fibre stress σ_{fd} at p_d results in maximum possible fibre pre-stress σ_{f0}, and consequently in maximum possible liner compressive stress σ_{00}, giving minimum hoop stress at any applied pressure p. It follows that this condition also produces lowest *equivalent stress* in the liner and therefore would be associated with the best possible fatigue resistance for the design.

To complete the analysis *equivalent stress* in the elastic range is given by von Mises equation (1.2), substituting σ_e for Y

$$2\sigma_e^2 = (\sigma_\theta - \sigma_l)^2 + (\sigma_l - \sigma_r)^2 + (\sigma_r - \sigma_\theta)^2 \tag{1.21}$$

Equivalent stress is useful in assessing liner cyclic fatigue performance.

1.7 Autofrettage theory

Autofrettage is important in producing pre-stresses σ_{00} and σ_{f0} in liner and fibre, respectively. The preceding elastic theory in Section 1.6 developed expressions for these pre-stresses necessary to give the required design performance. However, the actual provision of the correct pre-stresses depends on achieving the requisite amount of plastic strain in autofrettage, and therefore the latter process is an essential part of any rigorous hoop-wrapped cylinder design theory.

Figure 1.3 shows the autofrettage cycle for liner and fibre with an idealized non-strain-hardening liner in plane stress. Though not strictly valid for the triaxial stress state of this theory, the figure provides a helpful analogy in visualizing the mechanics of the autofrettage process. With respect to Fig. 1.3 the process is seen to comprise two distinctly different stages: firstly pressurizing the cylinder to cause initial liner yield, involving elastic deformation of both liner and fibre, followed by plastic straining of the liner around the von Mises locus to a 'conditioning' point where, on pressure release, the required pre-stresses σ_{00} and σ_{f0} are permanently locked into the cylinder for subsequent elastic operation in service.

For a strain-hardening material of initial yield strength Y_0, equal to the constant yield stress of Fig. 1.3, the initial loading line up to and including first yield would be identical, but thereafter in the plastic stage the effect of strain-hardening would be progressively to increase current yield stress Y above Y_0, and thus increase the pressure required to produce the same pre-stresses $\sigma_{\theta 0}$ and σ_{f0}.

In the following theory development the initial yielding stage is considered first, followed by analysis of the plastic strain stage for a non-strain-hardening material, and

finally the theory is adapted for treatment of a strain-hardening material.

1.7.1 Initial liner yielding

Yielding will occur when the principal stresses in the elastic stage of first pressurization reach an intensity satisfying the von Mises yield criterion, and the pressure at which this state occurs will be initial yield pressure p_{y0}. Equation (1.15) gives the elastic hoop stress $\sigma_\theta = Z \cdot p$, longitudinal stress is given by $\sigma_l = K \cdot p$, and mean radial stress $\sigma_r = A \cdot \sigma_\theta - (1 - A) \cdot p$. Therefore all three liner stresses are expressible in terms of general pressure p. Substituting these values into the yield criterion of equation (1.2), putting $Y = Y_0$, provides pressure p_{y0}, thus

$$p_{y0} = Y_0\{Z^2 + K^2 + [A(Z + 1) - 1]^2 - Z \cdot K - (Z + K)[A(Z + 1) - 1]\}^{-1/2} \qquad (1.22)$$

Having established liner initial yield pressure p_{y0}, corresponding values of liner stresses σ_θ, σ_l, and σ_r follow. Fibre stress σ_f at first yield is obtained via equation (1.18) putting $\sigma_{f0} = 0$.

1.7.2 Autofrettage pressure for non-strain-hardening liner

Figure 1.3 shows for the liner the elastic unloading stress–pressure line from the autofrettage conditioning point. Following unloading, re-pressurization would take place along precisely this same line, which has been characterized by equations developed in Section 1.6, until re-yielding occurs at a pressure $p_a > p_{y0}$. Therefore, as in the case of initial yielding, all three liner principal stresses are definable in terms of general pressure p, i.e. hoop stress

$\sigma_0 = Z \cdot p + \sigma_{\theta 0}$ from equation (1.17), longitudinal stress $\sigma_l = K \cdot p$, radial stress $\sigma_r = A \cdot \sigma_\theta - (1 - A) \cdot p$. The autofrettage pressure evaluation thus essentially follows that described for initial yielding in Section 1.7.1, substituting into von Mises yield criterion with constant yield stress Y and letting $p = p_a$, the autofrettage pressure, in the above stress expressions. Although a general closed-form solution for p_a is possible by this route, the result is unwieldy and not recommended for applied use. Instead, a better approach is to first insert known numerical values for Z, K, A, and $\sigma_{\theta 0}$ into the above expressions for σ_θ, σ_l, and σ_r, and *then* solve von Mises' equation (1.2). The resulting quadratic in p_a gives the autofrettage pressure required to produce liner and fibre pre-stresses $\sigma_{\theta 0}$ and σ_{f0}, respectively.

Liner principal stresses σ_θ, σ_l, and σ_r at pressure p_a follow, and corresponding fibre stress σ_f is given by equation (1.18).

An interesting feature of the above derivation for autofrettage pressure is that although significant plastic strain is involved in shifting the yield point around the von Mises locus, the final result is obtained without any consideration of strain whatsoever. This is not the case for a strain-hardening material, as shown in the following section.

1.7.3 Autofrettage pressure for a strain-hardening liner

Figure 1.6 is a simplified plane stress analogy illustrating the effect of liner strain hardening. Elastic lines a and b represent pre- and post-autofrettage, respectively. Two yield loci are shown, one representing initial yield stress Y_0, and the other current yield stress Y, expansion of the locus from Y_0 to Y being due to strain-hardening. Initial loading takes place along line a, with initial yielding at

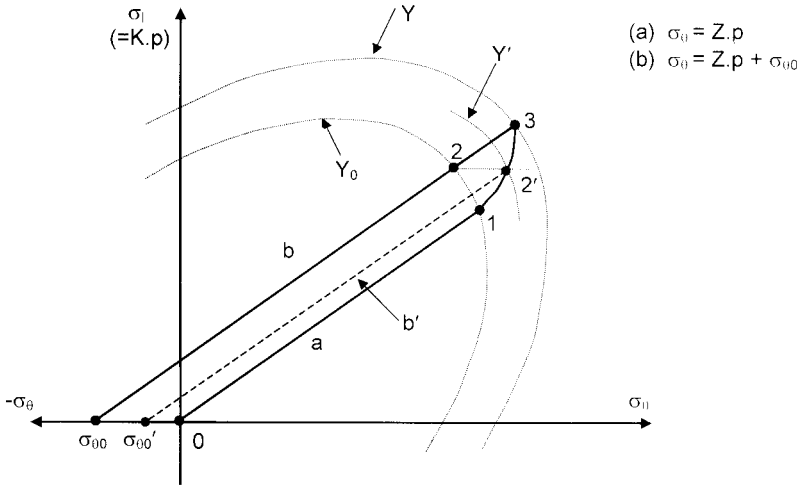

Fig. 1.6 Plane stress analogy of strain-hardening in autofrettage

point 1. For a given liner pre-stress $\sigma_{\theta 0}$, the autofrettage plastic strain path for a non-strain-hardening material would be $1 \rightarrow 2$ along the Y_0 locus resulting in (analogy) autofrettage pressure σ_{l2}/K. The exact triaxial analysis for this condition is given in Section 1.7.2. For a strain-hardening liner the strain path would not be $1 \rightarrow 2$ but $1 \rightarrow 3$, so as to accommodate the extension of line b necessary for preserving pre-stress $\sigma_{\theta 0}$. In consequence, autofrettage pressure for the analogy is increased to σ_{l3}/K. Of special note, if the non-strain-hardening autofrettage pressure was applied to the strain-hardening liner, the strain path would terminate at $2'$ corresponding to intermediate yield stress Y', and on elastic recovery along line b' the resulting pre-stress would be $\sigma'_{\theta 0}$, where numerically $\sigma'_{\theta 0} < \sigma_{\theta 0}$. It follows that in subsequent service the liner would be operating at an *actual* hoop stress greater than that intended in design.

The basic approach to analysis is similar to that for the non-strain-hardening liner of Section 1.7.2 except that the

triaxial stress equivalent of point 3 in Fig. 1.6 is initially unknown, and requires a method of successive approximation, applying plastic stress–strain increment theory to deduce current yield stress Y. Techniques applied in this procedure are described below, and step by step calculations are given in Sections 2.1 and 2.2.

1.7.3.1 Determination of permanent plastic hoop strain

This quantity is key to evaluating *equivalent strain*, which in turn governs current yield stress and hence autofrettage pressure.

Figure 1.7 shows the hoop stress–strain relationships for liner and fibre during the autofrettage cycle. Initial liner yield occurs at point 1 (equivalent to point 1 in analogy Fig. 1.6), and total hoop strain at the conditioning point (point 3 in analogy Fig. 1.6) is $\varepsilon_{\theta t}$. In estimating strain hardening, residual permanent plastic strain $\varepsilon_{\theta p}$, at $\sigma_\theta = 0$, is of interest. From Fig. 1.7 $\varepsilon_{\theta p} = \varepsilon_{\theta t} - \varepsilon_{\theta r}$, where $\varepsilon_{\theta r}$ is elastic recovery to the state $\sigma_\theta = 0$. Although this route to establishing $\varepsilon_{\theta p}$ is possible, it is complicated by the Poisson's ratio effect involving all three liner principal stresses, and a more simple and direct way is to work in terms of uniaxial fibre stress σ_f to deduce hoop strain at points of interest. Thus, from the equality of hoop strain, $\varepsilon_{\theta p}$ is equal to the fibre strain ε_f at $\sigma_\theta = 0$ post-autofrettage, and equations (1.17) and (1.18) can be brought to bear as follows:

From equation (1.17), pressure p at $\sigma_0 = 0$ is $p = -\sigma_{\theta 0}/Z$, and from equation (1.18) fibre stress σ_f at $\sigma_0 = 0$ is therefore, $\sigma_f = -(X/Z)\sigma_{\theta 0} + \sigma_{f0}$, (noting that σ_{00} is a negative quantity.) Thus, $\varepsilon_{\theta p} = \varepsilon_f = \sigma_f/E_f$, or

$$\varepsilon_{\theta p} = \frac{1}{E_f}\left[\sigma_{f0} - \left(\frac{X}{Z}\right)\sigma_{\theta 0}\right] \tag{1.23}$$

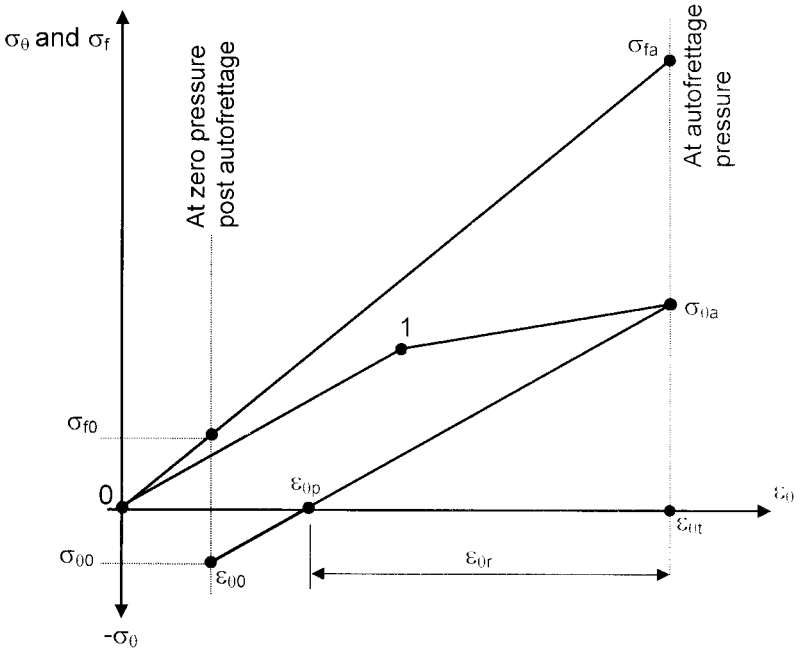

Fig. 1.7 Liner hoop and fibre stress versus strain in autofrettage

Equation (1.23) informs that permanent plastic hoop strain is a function only of design pre-stresses and design constants, and is totally unaffected by strain-hardening. For any given design $\varepsilon_{\theta p}$ can therefore be considered a constant.

1.7.3.2 Determination of equivalent permanent strain and strain-hardened yield stress

Equivalent strain is a plasticity concept defining that strain in simple tension producing the same amount of plastic work per unit material volume as all the principal stresses and strains in the complex system under consideration. The concept is useful for assessing strain hardening in autofrettage by converting the process strain to the equivalent in simple tension.

General equations relate strains to stresses in the plastic state, and in the nomenclature of this theory appear as

$$\frac{\delta\varepsilon_{\theta p}}{\sigma'_{\theta}} = \frac{\delta\varepsilon_{lp}}{\sigma'_{l}} = \frac{\delta\varepsilon_{rp}}{\sigma'_{r}} = \frac{\delta\varepsilon_{ep}}{\sigma'_{e}}$$

where $\delta\varepsilon$ denotes a strain increment, and σ' denotes a mean deviatoric stress over the strain increment, σ_e and ε_e referring to *equivalent* stress and strain, respectively.

Of the principal plastic strains only $\delta\varepsilon_{\theta p}$ is known immediately, as given by equation (1.23). Deviatoric equivalent stress σ'_e can be written $\frac{2}{3}\sigma_e$, and in the plastic range $\sigma_e = Y$. Deviatoric stress σ_θ can be written in terms of all three principal stresses as $\sigma'_\theta = [2\sigma_\theta - (\sigma_l + \sigma_r)]/3$. The resulting equation linking *equivalent* strain to known permanent hoop strain is thus

$$\frac{\delta\varepsilon_{ep}}{Y_m} = \frac{2\varepsilon_{\theta p}}{2\sigma_{\theta m} - (\sigma_{lm} + \sigma_{rm})} \tag{1.24}$$

In equation (1.24) all stresses are *mean* values over the strain increment, and therefore an evaluation of *equivalent strain* $\delta\varepsilon_{ep}$ is possible only when the full complement of stresses σ_θ, σ_l, σ_r, and Y are known at the start and finish of the increment. Starting stresses are known from the initial yielding theory of Section 1.7.1, but finishing stresses are generally unknown because of the strain-hardening; however, they are known for the special case of zero strain-hardening analysed in Section 1.7.2. Therefore the successive approximation procedure commences with this latter condition and proceeds as follows:

Mean values of all stresses over non-strain-hardening autofrettage are deduced from Sections 1.7.1 and 1.7.2

and together with permanent hoop strain ε_{0p} from equation (1.23) are inserted into equation (1.24) to provide a first approximation to *equivalent strain*, say $\delta\varepsilon_{ep1}$. A corresponding value for current yield stress, say Y_1, is read from the tensile stress–strain curve for the liner material.

Using $Y = Y_1$, the theory of Section 1.7.2 is applied to deduce a new (higher) autofrettage pressure, say p_{a1}, and the corresponding liner principal stresses, say σ_{0l}, σ_{ll}, and σ_{rl}, are evaluated. Mean values of all stresses, including yield stress $Y_m = (Y_0 + Y_1)/2$, are inserted into equation (1.24) and a second approximation to *equivalent strain*, say $\delta\varepsilon_{ep2}$, obtained, and hence a corresponding value for current yield stress, say Y_2.

The above procedure is repeated until successive values of Y are the same within acceptable error. Usually two or three calculation 'rounds' suffice.

1.7.3.3 Autofrettage pressure and associated stresses

Use of the final value of current yield stress Y emergent from the above procedure in the theory of Section 1.7.2 provides autofrettage pressure p_a and associated stress σ_0, σ_l, and σ_r. Corresponding fibre stress σ_f is given by equation (1.18).

A ready check on the validity of the calculated autofrettage pressure is afforded by knowledge of fibre pre-stress σ_{f0}, which gives direct access to the required diametrical (hoop) expansion δD of the actual cylinder measurable on completion of the autofrettage process, i.e.

$$\frac{\delta D}{D} = \frac{\sigma_{f0}}{E_f} \tag{1.25}$$

1.8 Theoretical strains

Over the pressure range of manufacture and use three strains are of interest, namely, fibre strain ε_f, liner hoop strain ε_θ, and liner longitudinal strain ε_l. Fibre strain is fully elastic over this pressure range, and therefore readily calculable once pressure at the point, or points, is known. Following autofrettage the two liner strains, ε_θ and ε_l, caused by pressurization are also fully elastic within the use pressure range, and can be evaluated once the three principal stresses, σ_θ, σ_l, and σ_r, are known for the point, or points, of interest. During autofrettage the liner undergoes three stages of straining: firstly elastic straining to initial yield, then plastic straining to the 'conditioning' point, and finally elastic recovery to zero pressure. Total directional strain present in the liner during subsequent use therefore comprises two components, pre-strain, and elastic strain from use pressurization.

Figure 1.7 shows hoop strain ε_θ–hoop/fibre stresses over the manufacture/use range. The liner plastic phase during autofrettage is shown as represented by rising hoop stress, but this depends on strain hardening, as indicated in Fig. 1.6, and anyway does not influence the theoretical outcome. Residual hoop strain $\varepsilon_{\theta 0}$ is less than permanent plastic strain $\varepsilon_{\theta p}$ because of liner elastic compression by the fibre.

During autofrettage the liner is in a plastic state, and permanent strain occurs not only in the hoop direction but in the longitudinal direction also.

1.8.1 Strain in fibre

As the fibre is elastic, and uniaxially loaded, fibre strain ε_f is directly proportional to fibre stress σ_f

$$\varepsilon_f = \frac{\sigma_f}{E_f} \tag{1.26}$$

where $\sigma_f = X \cdot p$ in pre-autofrettage loading, and $\sigma_f = X \cdot p + \sigma_{f0}$ post-autofrettage [from equation (1.18)]. Similarly fibre strain increment $\delta\varepsilon_f$ between two pressure points $p_1 \rightarrow p_2$ is given by

$$\delta\varepsilon_f = \frac{1}{E_f}(\sigma_{f2} - \sigma_{f1}) \tag{1.27}$$

1.8.2 Elastic strains in liner

Between any two points of pressure $p_1 \rightarrow p_2$ liner elastic strain increment is given by the general equations:

Hoop strain increment

$$\delta\varepsilon_{\theta e} = \frac{1}{E_l}\left[\left\{\sigma_{\theta 2} - \nu(\sigma_{l2} + \sigma_{r2})\right\} - \left\{\sigma_{\theta 1} - \nu(\sigma_{l1} + \sigma_{r1})\right\}\right] \tag{1.28}$$

Longitudinal strain increment

$$\delta\varepsilon_{le} = \frac{1}{E_l}\left[\left\{\sigma_{l2} - \nu(\sigma_{\theta 2} + \sigma_{r2})\right\} - \left\{\sigma_{l1} - \nu(\sigma_{01} + \sigma_{r1})\right\}\right] \tag{1.29}$$

where $\sigma_l = K \cdot p$, and $\sigma_r = A \cdot \sigma_\theta - (1 - A) \cdot p$ from equation (1.1). Hoop stress $\sigma_0 = Z \cdot p$ from equation (1.15) for pre-autofrettage, and $\sigma_\theta = Z \cdot p + \sigma_{\theta 0}$ post-autofrettage [from equation (1.17)].

It is noted that a simpler route to hoop strain increment $\delta\varepsilon_{\theta e}$ than equation (1.28) is given via fibre strain increment in equation (1.27), applying the hoop/fibre strain equality condition.

1.8.3 Plastic strains in liner

Liner plastic hoop strain $\varepsilon_{\theta p}$ was derived in Section 1.7.3.1 as equation (1.23). Knowing $\varepsilon_{\theta p}$, the general stress–plastic strain increment equations provide an expression for longitudinal plastic strain ε_{lp}

$$\varepsilon_{lp} = \left[\frac{2\sigma_{lm} - (\sigma_{rm} + \sigma_{\theta m})}{2\sigma_{\theta m} - (\sigma_{lm} + \sigma_{rm})}\right]\varepsilon_{\theta p} \tag{1.30}$$

where principal stresses $\sigma_{\theta m}$, σ_{lm}, and σ_{rm} are *mean* values over the strain increment corresponding to pressure increase $p_{y0} \rightarrow p_a$ as already deduced in Section 1.7.3.

1.8.4 Total strains in liner post-autofrettage

These are generally the sum of elastic and plastic strains in the direction of interest. Total hoop strain $\varepsilon_{\theta t}$ at any given pressure $p \leq p_a$ is given by the sum of $\varepsilon_{\theta p}$ from equation (1.23) and $\delta\varepsilon_{\theta e}$ from equation (1.28). Corresponding total longitudinal strain ε_{lt} is ε_{lp} from equation (1.30) + $\delta\varepsilon_{le}$ from equation (1.29). Some care is required in applying elastic strain equations (1.28) and (1.29) in the post-autofrettage situation, because at zero pressure the liner already contains hoop and longitudinal elastic strains superimposed on permanent plastic strains, locked in from the autofrettage process. The total directional elastic strain present at subsequent pressurization in service is therefore the algebraic sum of the locked-in strain plus that resulting from service pressure. Unless there is particular interest in evaluating these two components separately, the best approach to total elastic strain via equations (1.28) and (1.29) is to select the pre-autofettage zero pressure point as the origin for calculation (i.e. suffix 1), where it is positively known that all liner principal stresses, σ_θ, σ_l, and σ_r, are zero.

However, it is noted that a simpler more direct route to total *hoop* strain ε_{0t} is via fibre strain ε_f as given by equation (1.26), invoking the strain equality condition.

1.9 Estimating liner current yield stress at cylinder burst

Cylinder burst theory developed in Sections 1.3.3, 1.4, and 1.5 depends on current yield stress for quantitative evaluations. As most liner materials exhibit some degree of strain-hardening, current yield stress Y at the point of burst will generally exceed initial yield stress Y_0. This section investigates, and gives methods for estimating, the amount of plastic strain inherent in the burst process, and thus deriving the current yield stress for inclusion in burst theory.

Von Mises plane stress analogy Fig. 1.1c is used for visualizing general strain-hardening trends in the triaxially stressed cylinder. In Fig. 1.1c for a non-strain-hardening liner, bursting of the unwrapped cylinder is represented at point 1, and the critical burst condition for the wrapped cylinder at point 5. Over the range $1 \rightarrow 5$ fibre area and burst pressure increase progressively, but all bursts in the range are characterized by hoop failure, in which the fibre reaches maximum tensile strength and fractures, resulting in liner failure by pressure overload. This is the case because commonly used ductile metallic liners are capable of greater total strain to failure than are commonly used high-strength fibres. However, unless there is practical evidence to support this, as a general check it is recommended that calculated liner *equivalent* plastic strain corresponding to fibre failure strain as derived from

Section 1.9.2 does not significantly exceed uniform plastic strain *prior to* neck formation measured in the liner tensile test.

Note
An exception to the above general progression of fibre fracture followed by liner hoop burst, could in theory occur with very low amounts of fibre reinforcement, where the liner may be capable of developing sufficient strength through strain hardening to survive the pressure at which fibre fracture took place. However this situation is largely academic, since in practice the object of overwrapping will be to add sufficient fibre to significantly increase burst pressure.

1.9.1 Liner plastic hoop strain at burst

The fibre mechanical property of remaining elastic to fracture provides the constant hoop strain at burst for all hoop mode bursts over the range 1 → 5 in Fig. 1.1c, thus

$$\varepsilon_f = \varepsilon_{\theta t} = \frac{T_f}{E_f}$$

From a strain-hardening aspect it is the liner plastic strain, $\varepsilon_{\theta p}$, part of this total hoop strain which is of interest; this is given by

$$\varepsilon_{\theta p} = \varepsilon_{\theta t} - \varepsilon_{\theta e}$$

where $\varepsilon_{\theta e}$ is the elastic component of the total strain given by

$$\varepsilon_{\theta e} = \frac{1}{E_l}[\sigma_\theta - \nu(\sigma_l + \sigma_r)]$$

Thus, plastic hoop strain at burst is given by

$$\varepsilon_{\theta p} = \frac{T_f}{E_f} - \frac{1}{E_l}[\sigma_\theta - \nu(\sigma_l + \sigma_r)] \tag{1.31}$$

where σ_θ, σ_l, and σ_r are liner stresses at burst.

Returning to Fig. 1.1c, it is clear that as fibre reinforcement area increases, corresponding to anticlockwise rotation around the yield locus, the general trend is for σ_θ to decrease and σ_l to increase. Now since σ_r is small compared with σ_θ and σ_l, the corresponding trend given by equation (1.31) is for $\varepsilon_{\theta p}$ to increase as fibre area and burst pressure increase.

Note

Both equations (1.31) and (1.23) are expressions for plastic strain $\varepsilon_{\theta p}$. However, these two expressions should not be construed as interchangeable because they relate to two fundamentally different conditions of cylinder behaviour. Equation (1.31) is concerned with plastic hoop strain developed in the liner up to the point of hoop bursting, upon which event internal pressure p and all stresses (σ_θ, σ_l, and σ_r in liner, σ_f in fibre) are dissipated to zero. By contrast equation (1.23) is concerned with plastic hoop strain developed in the autofrettage process, a quantity that is, as shown in Section 1.7.3.1, equal to the common hoop strain residing in fibre and liner following autofrettage, at a point when liner hoop stress σ_θ is zero but p exceeds zero, meaning that neither $\sigma_l (= K \cdot p)$ nor $\sigma_r (= A \cdot \sigma_\theta - (1 - A) \cdot p)$ are zero at the point.

1.9.2 Liner equivalent plastic strain at burst

Knowledge of this quantity leads directly to current yield stress.

Although equation (1.24) was developed as part of autofrettage analysis, it is a general equation for *equivalent* plastic strain ε_{ep} in terms of plastic hoop strain $\varepsilon_{\theta p}$ and *mean* principal stresses over the strain increment, and equally applicable to plastic strain associated with bursting. Considering the denominator of this expression, $2\sigma_{\theta m} - (\sigma_{lm} + \sigma_{rm})$ in conjunction with Fig. 1.1c, ignoring the effect of changes in small σ_r, it is observed that as fibre area and burst pressure increase, $\sigma_{\theta m}$ decreases and σ_{lm} increases, with the net result that the denominator of equation (1.24) decreases. This, coupled with the deduced trend for $\varepsilon_{\theta p}$ from Section 1.9.1, implies that *equivalent* strain ε_{ep}, and therefore current yield stress Y, will *increase* as fibre reinforcement increases from $a_f = 0$ to $a_f = a_{fc}$. It is clear that since liner *equivalent* strain depends on plastic hoop strain, which in turn is mainly influenced by fibre strain to failure, fibre modulus will be a major influence in controlling liner general plastic strain and therefore current yield stress at burst.

1.9.3 Procedure for estimating liner current yield stress

At the very start of design to this theory it is important to establish the true current yield stress, both at *critical* burst, since this fixes liner wall thickness, and at *design* burst, since this fixes fibre reinforcement area. Once these two principal design variables are set, the remainder of the design process follows. The successive approximation procedure for establishing each is essentially the same, namely:

1. Start with a first estimate yield stress for the burst condition of interest.
2. Deduce liner plastic hoop strain at burst.

3. Convert the hoop strain from point 2 into an *equivalent* strain.
4. Use *equivalent* strain from point 3 in conjunction with liner mechanical property data to establish a corresponding yield stress.
5. Compare the yield stress from point 4 with that in point 1. If the same (within allowed tolerance), task is complete. If not the same, use yield stress from point 4 as representative and repeat processes 2 → 5.

Usually two 'rounds' of the process are sufficient to fix current yield stress. Detailed steps in the process are given below.

1.9.3.1 Critical burst

The natural start point to proceedings is the *critical* burst condition since this involves greatest strain and therefore has current yield stress Y closest to tensile strength T_l. Therefore to start, assume $Y = T_l$ and solve equation (1.9) to obtain A, giving a first wall thickness t for the prescribed *critical burst* pressure p_{bc}. Longitudinal stress $\sigma_l = K \cdot p_{bc}$, hence radial stress σ_r follows from equation (1.6), and hoop stress σ_θ from equation (1.7), giving all three principal stresses at *critical burst*.

Use σ_θ in equation (1.10) to establish the fibre reinforcement a_{fc} necessary to give *critical burst*. (a_{fc} is used in succeeding calculations, though never actually in the designed and manufactured cylinder.)

Solve equation (1.31) to obtain plastic hoop strain $\varepsilon_{\theta p}$.

Deduce coefficient Z associated with equation (1.15), putting $a_{fc} = a_f$, and hence solve equation (1.22) for initial yield pressure p_{y0} corresponding to fibre area a_{fc}. Evaluate principal stresses σ_θ, σ_l, and σ_r at p_{y0}.

Convert plastic hoop strain $\varepsilon_{\theta p}$ to equivalent strain ε_{cp} applying equation (1.24), using *mean* values of σ_θ, σ_l, σ_r,

and Y over the strain increment corresponding to $p_{y0} \rightarrow p_{bc}$.

Obtain current yield stress Y corresponding to ε_{ep} from the liner's tensile stress–strain mechanical property data (see following note). This point of calculation corresponds to point 5 above. Continue as appropriate.

1.9.3.2 Design burst

Since *design* burst is at lower pressure, and therefore involves less plastic strain than the *critical* burst, current yield stress evaluated for the latter (as described above) is used as the starter Y. Also a firm and final value of wall thickness parameter A corresponding to this yield stress was derived from equation (1.9) as part of the procedure. Starting from this position:

For prescribed *design burst* pressure p_{bd} solve equation (1.11a) for hoop stress σ_θ at *design* burst. Derive companion stresses, σ_l and σ_r at *design* burst.

Use σ_θ in equation (1.12a) to establish the fibre reinforcement a_{fd} necessary to give *design* burst p_{bd}.

Solve equation (1.31) to obtain plastic hoop strain $\varepsilon_{\theta p}$.

Deduce coefficient Z associated with equation (1.15), putting $a_{fd} = a_f$, and hence solve equation (1.22) for initial yield pressure p_{y0} corresponding to fibre area a_{fd}. Evaluate principal stresses σ_θ, σ_l, and σ_r at p_{y0}.

Convert plastic hoop strain $\varepsilon_{\theta p}$ to equivalent strain ε_{cp} using equation (1.24), ensuring that *mean* values of $\sigma_\theta, \sigma_l, \sigma_r$, and Y are used over the strain increment corresponding to $p_{y0} \rightarrow p_{bd}$.

Obtain current yield stress Y corresponding to ε_{ep} from the liner's tensile stress–strain mechanical property data (see following note). This point of calculation corresponds to point 5 above. Continue as appropriate.

Note

The stress–strain mechanical property data referred to are the data obtained in the tensile test from initial yield (or proof stress) up to the point of maximum load, which corresponds to the range of *uniform* elongation, prior to the start of neck formation. Only permanent plastic strain is of interest, and if strain readings from the testing machine include an elastic component the latter should be zeroed out from the data. For commonly used liner materials *uniform* elongation will typically be no more than one-half of the total elongation for a proportional gauge-length specimen. Because of the relatively low strain hardening of these liner materials with Y_0/T_1 typically ≈ 0.9, the plastic stress–strain curve of interest can be adequately represented by a simple mathematical model, once initial yield stress, tensile strength, and uniform strain to maximum load-point are known. Such a model is derived in Annex 3 and is used in the examples in Part 2 which illustrate the use of the design theory.

Part 2

Application of the theory

The most practical way to demonstrate application is to theoretically evaluate actual hoop-wrapped cylinders for which independently obtained test results are known. For this purpose results from an extensive experimental programme conducted by Alcoa Laboratories in the mid-1980s (**1**), are drawn upon.

The Alcoa experiments were based on 13 inch (330 mm) diameter liners, nominally 0.5 inch (12.7 mm) wall thickness, overwrapped with E-glass fibre in a polyester resin matrix, the composite cylinders being for use as CNG (compressed natural gas) fuel tanks at 3000 lb/in^2 nominal service pressure. Two sets of experiments were carried out involving 26 cylinders. In one set, the autofrettage process was investigated by subjecting liners with differing amounts of reinforcement to a common autofrettage conditioning pressure, and measuring stresses/strains occurring as a result. In the other set, cylinder bursting was investigated, and in particular the critical condition where burst mode changes from hoop to longitudinal with increasing fibre reinforcement.

All experimental results by Alcoa were presented in 'imperial' units. However, as it is now increasingly the convention to work in international 'metric units', test results have been converted into metric for comparison with this theory.

The theory is first applied to the actual cylinders produced and tested by Alcoa, to demonstrate accuracy of prediction; the theory is then used to design from basics a cylinder meeting the Alcoa burst pressure specification.

2.1 Comparison of theory with experiment

All test data in this section are from the Alcoa paper except where otherwise noted.

2.1.1 Cylinder details

2.1.1.1 Aluminium liner

- Material: alloy 6061.
- Mechanical properties:
  - yield stress, 276 MPa;
  - tensile strength, 324 MPa (see note);
  - tensile modulus, 69×10^3 MPa;
  - Poisson's ratio, 0.3.
- Dimensions:
  - external diameter, 330.2 mm;
  - wall thickness, 12.75 mm.

Note
The tensile strength given by Alcoa is 41.6×10^3 lb/in^2 equivalent to 287 MPa, at 16 percent elongation. Alcoa arrived at this figure by manipulation of mathematically generated stress–strain curves, and it is believed to be in error. By comparison, standard BS 5045:3 gives yield/tensile properties for alloy 6061 as 280/325 MPa respectively, a range common to several 'Series 6000' alloys used for gas cylinders. For this reason tensile strength for the Alcoa cylinder has been put at 324 MPa, since an accurate value of this property is essential to theoretical predictions.

2.1.1.2 Overwrap

Fibre

- Material: E-glass.

- Mechanical properties:
  - tensile strength, (impregnated strand) 1724 MPa;
  - tensile modulus, 72.4×10^3 MPa.

Resin

- Material: polyester.
- Mechanical properties:
  - tensile strength, 29 MPa;
  - tensile modulus, 1.17×10^3 MPa;
  - ultimate elongation, 30 percent.

2.1.1.3 Overwrapped cylinder pressures

- Nominal service pressure: 207 bar.
- Required minimum burst pressure: 517 bar.
- Autofrettage pressure (where applied): 400 bar.

2.1.2 Cylinder burst evaluations

2.1.2.1 Experimental results

Figure 2.1 is a conversion from Fig. 13 of the Alcoa paper showing experimental burst pressure versus fibre reinforcement area. Six data points are shown, each covering three separate cylinder tests. Three of the data points, numbers 1, 2, and 3, represent hoop bursts, and three, numbers 4, 5, and 6, represent longitudinal bursts. A further data point, 7, represents the unwrapped cylinder ($a_f = 0$). A striking feature of the data is the completely flat characteristic once critical burst pressure is attained, further reinforcement providing no further pressure increase. By converging the two burst trend lines Teply and Herbein estimated that a *critical* burst pressure p_{bc} of 563 bar occurred with fibre area 8.7 mm^2/mm.

Data point number	*Fibre area a_f (mm^2/mm)*	*Burst pressure p_b (bar)*
1	2.59	379
2	4.93	480
3	7.39	530
4	10.34	563
5	12.45	563
6	14.94	563
Estimated p_{bc}	8.7	563
7 (unwrapped)	0	276

Note, a_f = total fibre area both sides.

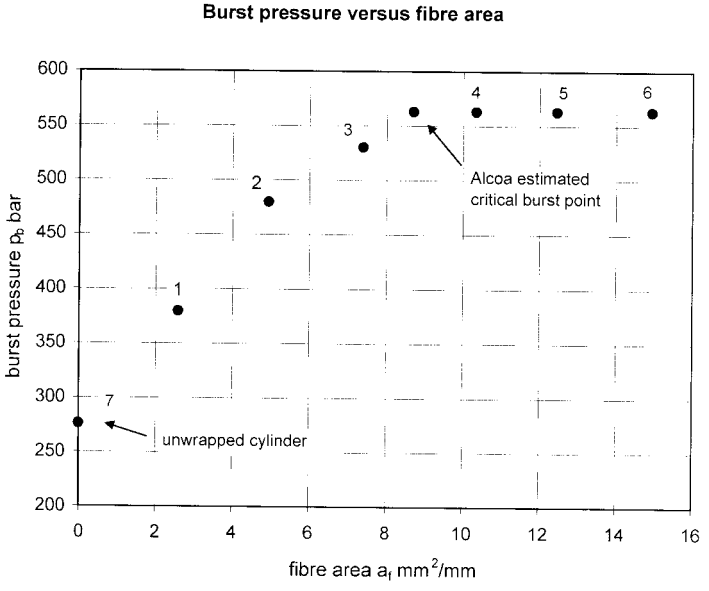

Fig. 2.1 Alcoa experimental burst test results

2.1.2.2 Theoretical results

The general procedure is to first evaluate the critical burst condition, because this will be associated with maximum plastic strain and therefore highest yield stress, and then use the emergent yield stress as the first approximation to that in the highest pressure hoop burst under consideration, and so on to evaluate fibre areas at various descending hoop burst pressures affording comparison with Fig. 2.1.

The plastic stress–strain model developed in Annex 3 requires a value for maximum uniform strain in the tensile test. While the Alcoa paper quotes an 'ultimate strain' of 16 percent, it is not clear if this was measured on a proportional gauge length. Because of this uncertainty, elongation of 12 percent from BS5045:3 is used, and it is assumed that the *uniform* component of this elongation is one-half of the total, namely 6 percent. The resulting Y–ε_{cp} model is

$$Y = 324[0.85 + 5(\varepsilon_{cp}) - 41.7(\varepsilon_{cp})^2]$$

1. Evaluation of the critical burst condition

From data in Section 2.1.1 liner geometric parameters are: $A = t/D = 0.0386$, $d = D - 2t = 304.7\,\text{mm}$, $K = d^2/(D^2 - d^2) = 5.73$.

Current yield stress Y at critical burst is initially unknown, because of strain-hardening, and solution follows the procedure of Section 1.9.3.1, first conducting a conditional evaluation on the basis of an assumed current yield stress value (taken as $Y = T_1$ because of the anticipated strain to failure), and then by subsequent analysis confirming that the assumption was correct. In the following worked calculations, steps (i), (ii), and (iii) cover the basic critical burst evaluation and steps (iv) to (x)

inclusive cover validation of the initially assumed yield stress used in the evaluation. (It so happens that a single round of calculations is sufficient to provide a solution. However, if this had not been the case, a further round would be conducted, starting with the new value of Y emergent from the previous round.)

(i) Assuming $Y = T_l = 324\,\text{MPa}$ for first approximation, equation (1.9) gives $p_{bc} = 567$ bar.

(ii) Principal liner stresses at p_{bc} are, following the evaluation procedure recommended in Section 1.3.3.2, after equation (1.9): $\sigma_l = K \cdot p_{bc} = 324.9$ MPa, σ_r from equation (1.6) $= -49\,\text{MPa}$, σ_θ from equation (1.7) $= 149\,\text{MPa}$.

(iii) From equation (1.10), putting $\sigma_\theta = 149\,\text{MPa}$ from (ii), fibre area at critical burst $a_{fc} = 7.82\,\text{mm}^2/\text{mm}$.

(iv) Applying equation (1.31), using stresses from (ii), liner plastic hoop strain $\varepsilon_{\theta p} = 2.3$ percent to failure at p_{bc}.

(v) Evaluating liner stress coefficient Z from the expression associated with equation (1.15), $Z = 9.41$.

(vi) Applying $Z = 9.41$ from (v) in equation (1.22), liner initial yield pressure $p_{y0} = 314.8$ bar.

(vii) Evaluating liner principal stresses at p_{y0}: $\sigma_\theta = Z \cdot p_{y0} = 296.2\,\text{MPa}$, $\sigma_l = K \cdot p_{y0} = 180.4\,\text{MPa}$, $\sigma_r = -18.8$ MPa from equation (1.1).

(viii) From (ii) and (vii) mean liner stresses over the strain increment corresponding to $p_{y0} \rightarrow p_{bc}$ are therefore: $\sigma_{\theta m} = 222.6\,\text{MPa}$, $\sigma_{lm} = 252.7\,\text{MPa}$, $\sigma_{rm} = -33.9$ MPa, and $Y_m = [(276 + 324)/2] = 300\,\text{MPa}$.

(ix) Putting $\varepsilon_{\theta p}$ from (iv) in equation (1.24), liner *equivalent* plastic strain $\varepsilon_{ep} = 6.1$ percent.

(x) From the tensile stress–strain model above, at $\varepsilon_{ep} = 6.1$ percent, $Y = 324\,\text{MPa}$, validating the initial assumption and hence the result of critical

burst pressure = 567 bar in step (i) is confirmed as correct.

Result:

- Critical burst pressure $p_{bc} = 567$ bar.
- Fibre reinforcement area to give p_{bc}, $a_{fc} = 7.82\,mm^2/mm$ (total both sides).

2. *Evaluation of fibre area to give a prescribed burst pressure of 500 bar*

(500 bar is selected as being just below the established *critical* burst pressure.)

The task is to determine the amount of fibre overwrap required on a liner of the prescribed size, to provide a hoop burst at 500 bar. As in evaluation 1 above, because of strain-hardening the current yield stress at bursting is initially unknown, and solution therefore follows the procedure of Section 1.9.3.2. Although the latter refers specifically to 'design burst', the procedure is generally applicable to all hoop bursts p_b, where $p_{bl} < p_b < p_{bc}$, and involves first a conditional evaluation on the basis of an assumed current yield stress confirmed by subsequent analysis. In the following worked calculations, steps (i) and (ii) cover the basic fibre area evaluation, and steps (iii) to (ix) inclusive cover validation of the assumed current yield stress. Two rounds of calculation are necessary to arrive at a correct solution.

For a first approximation, current yield stress at burst is assumed to be that at p_{bc}, i.e. $Y = 324$ MPa, on the basis that this represents a known upper bound.

(i) With respect to equation (1.11), associated expressions for constants m and n give: $m = 263$ MPa, and constant $n = -7.07 \times 10^3 (MPa)^2$. Hence, liner principal stresses at burst are: $\sigma_\theta = 287.6$ MPa from

equation (1.11), $\sigma_l = K \cdot p_b = 286.5\,\text{MPa}$, $\sigma_r = -37.0\,\text{MPa}$ from equation (1.1).

(ii) From equation (1.12), putting $\sigma_\theta = 287.6\,\text{MPa}$ from (i), for a 500 bar burst, fibre area $a_{fb} = 4.58\,\text{mm}^2/\text{mm}$.

(iii) From equation (1.31), liner plastic hoop strain $\varepsilon_{\theta p} = 2.07$ percent to hoop failure.

(iv) Evaluating liner stress coefficient Z from the expression associated with equation (1.15), $Z = 10.30$.

(v) Applying $Z = 10.30$ from (iv) in equation (1.22) liner initial yield pressure $p_{y0} = 292.1$ bar.

(vi) Evaluating liner principal stresses at p_{y0}: $\sigma_\theta = Z \cdot p_{y0} = 300.9\,\text{MPa}$, $\sigma_l = K \cdot p_{y0} = 167.4\,\text{MPa}$, $\sigma_r = -16.5\,\text{MPa}$ from equation (1.1).

(vii) From (i) and (vi) mean liner stresses over the strain increment corresponding to $p_{y0} \rightarrow p_b$ are therefore: $\sigma_{\theta m} = 294.2\,\text{MPa}$, $\sigma_{lm} = 226.9\,\text{MPa}$, $\sigma_{rm} = -26.7$ MPa, and $Y_m = [(276 + 324)/2] = 300\,\text{MPa}$.

(viii) Putting $\varepsilon_{\theta p}$ from (iii) in equation (1.24) liner *equivalent* plastic strain $\varepsilon_{ep} = 3.20$ percent.

(ix) From the tensile stress–strain model, at $\varepsilon_{ep} = 3.20$ percent, $Y = 313.3\,\text{MPa}$, indicating that the assumption of $Y = 324\,\text{MPa}$ made at the start of calculation is too high, and invalid, necessitating a further calculation round.

For a second approximation, current yield stress at burst is assumed that from the first approximation, i.e. 313.3 MPa.

(i) With respect to equation (1.11), associated expressions for constants m and n give: $m = 263\,\text{MPa}$, and constant $n = 0$. Hence, liner principal stresses at burst are: $\sigma_\theta = 263.0\,\text{MPa}$ from equation (1.11), $\sigma_l = K \cdot p_b = 286.5\,\text{MPa}$, $\sigma_r = -37.9\,\text{MPa}$ from equation (1.1).

(ii) From equation (1.12), putting $\sigma_\theta = 263.0$ MPa from (i), for a 500 bar burst, fibre area $a_{fb} = 4.95\,mm^2/mm$.

(iii) From equation (1.31), liner plastic hoop strain $\varepsilon_{\theta p} = 2.11$ percent to hoop failure.

(iv) Evaluating liner stress coefficient Z from the expression associated with equation (1.15), $Z = 10.19$.

(v) Applying $Z = 10.19$ from (iv) in equation (1.22) liner initial yield pressure $p_{y0} = 294.8$ bar.

(vi) Evaluating liner principal stresses at p_{y0}: $\sigma_\theta = Z \cdot p_{y0} = 300.4$ MPa, $\sigma_l = K \cdot p_{y0} = 168.9$ MPa, $\sigma_r = -16.7$ MPa from equation (1.1).

(vii) From (i) and (vi) mean liner stresses over the strain increment corresponding to $p_{y0} \rightarrow p_b$ are therefore: $\sigma_{\theta m} = 281.7$ MPa, $\sigma_{lm} = 227.7$ MPa, $\sigma_{rm} = -27.3$ MPa, and $Y_m = [(276 + 313.3)/2] = 294.7$ MPa.

(viii) Putting $\varepsilon_{\theta p}$ from (iii) in equation (1.24), liner *equivalent* plastic strain $\varepsilon_{ep} = 3.43$ percent.

(ix) From the tensile stress–strain model, at $\varepsilon_{ep} = 3.43$ percent, $Y = 315$ MPa. Since this value is close to the assumed value, $Y = 315$ MPa is taken as the current yield stress at $p_b = 500$ bar.

It remains to repeat steps (i) and (ii) of the procedure using $Y = 315$ MPa. Hence, from step (i) $m = 263.0$ MPa, $n = -1.1 \times 10^3 (\text{MPa})^2$, giving $\sigma_\theta = 267.1$ MPa, and from step (ii) using this value of σ_θ in equation (1.12) gives fibre reinforcement area $a_{fb} = 4.89\,mm^2/mm$ (total both sides).

3. Evaluation of fibre area to give a prescribed burst pressure of 400 bar

The procedure is exactly that of evaluation *2* above, two rounds of calculation being necessary to arrive at a correct solution. For a first approximation, current yield stress at burst is assumed to be that at $p_b = 500$ bar, i.e.

$Y = 315$ MPa from evaluation *2*, since this represents a known upper bound.

(i) With respect to equation (1.11), associated expressions for constants m and n give: $m = 210.4$ MPa, and constant $n = -37.8 \times 10^3$ (MPa)^2. Hence, liner principal stresses at burst are: $\sigma_\theta = 326.3$ MPa from equation (1.11), $\sigma_l = K \cdot p_b = 229.2$ MPa, $\sigma_r = -25.9$ MPa from equation (1.1).

(ii) From equation (1.12), putting $\sigma_\theta = 326.3$ MPa from (i), for a 400 bar burst, fibre area $a_{fb} = 2.24\,\text{mm}^2/\text{mm}$.

(iii) From equation (1.31), liner plastic hoop strain $\varepsilon_{\theta p} = 2.0$ percent to hoop failure.

(iv) Evaluating liner stress coefficient Z from the expression associated with equation (1.15), $Z = 11.07$.

(v) Applying $Z = 11.07$ from (iv) in equation (1.22) liner initial yield pressure $p_{y0} = 274.3$ bar.

(vi) Evaluating liner principal stresses at p_{y0}: $\sigma_0 = Z \cdot p_{y0} = 303.7$ MPa, $\sigma_l = K \cdot p_{y0} = 157.2$ MPa, $\sigma_r = -14.6$ MPa from equation (1.1).

(vii) From (i) and (vi) mean liner stresses over the strain increment corresponding to $p_{y0} \rightarrow p_b$ are therefore: $\sigma_{\theta m} = 315.0$ MPa, $\sigma_{lm} = 193.2$ MPa, $\sigma_{rm} = -20.3$ MPa, and $Y_m = [(276 + 315)/2] = 295.5$ MPa.

(viii) Putting ε_{0p} from (iii) in equation (1.24), liner *equivalent* plastic strain $\varepsilon_{ep} = 2.58$ percent.

(ix) From the tensile stress–strain model, at $\varepsilon_{ep} = 2.58$ percent, $Y = 308.2$ MPa, indicating that the assumption of $Y = 315$ MPa made at the start of calculation is too high, and invalid, necessitating a further calculation round.

For a second approximation, current yield stress at burst is assumed to be that from the first approximation, i.e. 308.2 MPa.

(i) With respect to equation (1.11), associated expressions for constants m and n give: $m = 210.4$ MPa, and constant $n = -33.4 \times 10^3$ (MPa)^2. Hence, liner principal stresses at burst are: $\sigma_\theta = 316.1$ MPa from equation (1.11), $\sigma_l = K \cdot p_b = 229.2$ MPa, $\sigma_r = -26.3$ MPa from equation (1.1).

(ii) From equation (1.12), putting $\sigma_\theta = 316.1$ MPa from (i), for a 400 bar burst, fibre area $a_{fb} = 2.39$ mm^2/mm.

(iii) From equation (1.31), liner plastic hoop strain $\varepsilon_{\theta p} = 2.01$ percent to hoop failure.

(iv) Evaluating liner stress coefficient Z from the expression associated with equation (1.15), $Z = 11.02$.

(v) Applying $Z = 11.02$ from (iv) in equation (1.22), liner initial yield pressure $p_{y0} = 275.5$ bar.

(vi) Evaluating liner principal stresses at p_{y0}: $\sigma_\theta = Z \cdot p_{y0} = 303.6$ MPa, $\sigma_l = K \cdot p_{y0} = 157.9$ MPa, $\sigma_r = -14.8$ MPa from equation (1.1).

(vii) From (i) and (vi) mean liner stresses over the strain increment corresponding to $p_{y0} \rightarrow p_b$ are therefore: $\sigma_{\theta m} = 309.9$ MPa, $\sigma_{lm} = 193.6$ MPa, $\sigma_{rm} = -20.6$ MPa, and $Y_m = [(276 + 308.2)/2] = 292.1$ MPa.

(viii) Putting $\varepsilon_{\theta p}$ from (iii) in equation (1.24), liner *equivalent* plastic strain $\varepsilon_{ep} = 2.63$ percent.

(ix) From the tensile stress–strain model, at $\varepsilon_{ep} = 2.63$ percent, $Y = 308.7$ MPa. Since this value is close to the assumed value, $Y = 309$ MPa is taken as the current yield stress at $p_b = 400$ bar.

It remains to repeat steps (i) and (ii) of the procedure using $Y = 309$ MPa. Hence, from step (i), $m = 210.4$ MPa, $n = -33.91 \times 10^3$ (MPa)^2, giving $\sigma_\theta = 317.3$ MPa, and from step (ii) using this value of σ_θ in equation (1.12) gives fibre reinforcement area $a_{fb} = 2.38$ mm^2/mm (total both sides).

4. Evaluation of fibre area to give a prescribed burst pressure of 350 bar

The procedure is exactly that of evaluations *2* and *3* above. Two rounds of calculation are made for completeness, but as will be seen the first round provides a result close enough to permit a good estimate. For a first approximation, current yield stress at burst is assumed to be that at $p_b = 400$ bar, i.e. $Y = 309$ MPa, from evaluation *3* since this represents a known upper bound.

(i) With respect to equation (1.11), associated expressions for constants m and n give: $m = 184.1$ MPa, and constant $n = -49.2 \times 10^3$ (MPa)^2. Hence, liner principal stresses at burst are: $\sigma_\theta = 332.2$ MPa from equation (1.11), $\sigma_l = K \cdot p_b = 200.6$ MPa, $\sigma_r = -20.8$ MPa from equation (1.1).

(ii) From equation (1.12), putting $\sigma_\theta = 332.2$ MPa from (i), for a 350 bar burst, fibre area $a_{fb} = 1.27$ mm^2/mm.

(iii) From equation (1.31), liner plastic hoop strain $\varepsilon_{\theta p} = 1.98$ percent to hoop failure.

(iv) Evaluating liner stress coefficient Z from the expression associated with equation (1.15), $Z = 11.43$.

(v) Applying $Z = 11.43$ from (iv) in equation (1.22) liner initial yield pressure $p_{y0} = 266.6$ bar.

(vi) Evaluating liner principal stresses at p_{y0}: $\sigma_\theta = Z \cdot p_{y0} = 304.7$ MPa, $\sigma_l = K \cdot p_{y0} = 152.8$ MPa, $\sigma_r = -13.9$ MPa from equation (1.1).

(vii) From (i) and (vi) mean liner stresses over the strain increment corresponding to $p_{y0} \rightarrow p_b$ are therefore: $\sigma_{\theta m} = 318.5$ MPa, $\sigma_{lm} = 176.7$ MPa, $\sigma_{rm} = -17.4$ MPa, and $Y_m = [(276 + 309)/2] = 292.5$ MPa.

(viii) Putting $\varepsilon_{\theta p}$ from (iii) in equation (1.24) liner *equivalent* plastic strain $\varepsilon_{ep} = 2.42$ percent.

(ix) From the tensile stress–strain model, at $\varepsilon_{ep} = 2.42$ percent, $Y = 306.7$ MPa. This is close enough to the assumed $Y = 309$ MPa to guess the actual current Y being around 307 MPa, but for completeness a second approximation is run as shown below.

For a second approximation, current yield stress at burst is assumed to be that from the first approximation, i.e. 306.7 MPa.

(i) With respect to equation (1.11), associated expressions for constants m and n give: $m = 210.4$ MPa, and constant $n = -47.73 \times 10^3$ (MPa)^2. Hence, liner principal stresses at burst are: $\sigma_\theta = 329.1$ MPa from equation (1.11), $\sigma_l = K \cdot p_b = 200.6$ MPa, $\sigma_r = -20.9$ MPa from equation (1.1).

(ii) From equation (1.12), putting $\sigma_\theta = 329.1$ MPa from (i), for a 350 bar burst, fibre area $a_{fb} = 1.32\,\text{mm}^2/\text{mm}$.

(iii) From equation (1.31), liner plastic hoop strain $\varepsilon_{\theta p} = 1.98$ percent to hoop failure.

(iv) Evaluating liner stress coefficient Z from the expression associated with equation (1.15), $Z = 11.41$.

(v) Applying $Z = 11.41$ from (iv) in equation (1.22) liner initial yield pressure $p_{y0} = 267.0$ bar.

(vi) Evaluating liner principal stresses at p_{y0}: $\sigma_\theta = Z \cdot p_{y0} = 304.6$ MPa, $\sigma_l = K \cdot p_{y0} = 153.0$ MPa, $\sigma_r = -13.9$ MPa from equation (1.1).

(vii) From (i) and (vi) mean liner stresses over the strain increment corresponding to $p_{y0} \rightarrow p_b$ are therefore: $\sigma_{\theta m} = 316.9$ MPa, $\sigma_{lm} = 176.8$ MPa, $\sigma_{rm} = -17.4$ MPa, and $Y_m = [(276 + 306.7)/2] = 291.4$ MPa.

(viii) Putting $\varepsilon_{\theta p}$ from (iii) in equation (1.24) liner *equivalent* plastic strain $\varepsilon_{ep} = 2.43$ percent.

(ix) From the tensile stress–strain model, at $\varepsilon_{cp} = 2.43$ percent, $Y = 306.8$ MPa. Since this value is almost the same as the assumed $Y = 306.7$ MPa, the latter is taken as the yield stress at $p_b = 350$ bar, and hence, from step (ii) above, corresponding fibre reinforcement $a_{fb} = 1.32\,mm^2/mm$ (total both sides).

2.1.2.3 *Comparison of theoretical and experimental burst results*

Figure 2.2 shows theoretical results for critical burst, and hoop bursts at 500, 400, and 350 bar superimposed on the Alcoa experimental results of Fig. 2.1.

As can be seen theory predicted the critical burst pressure very closely, within less than 1 percent of that measured. As Teply and Herbein noted, it is difficult to pinpoint the critical condition experimentally, and it is therefore inappropriate to draw too much from an estimated versus theoretical reinforcement comparison, except to say that both occur at around the same fibre area, with it would seem, theory slightly under-predicting.

In the hoop burst range, theory overestimates burst pressure by around 4–6 percent, the difference being least at higher burst pressures, i.e. > 500 bar, as would normally be designed for in practice.

2.1.3 Cylinder autofrettage evaluations

In the Alcoa experiments, Teply and Herbein took liners in accordance with Section 2.1.1, and overwrapped with three different amounts of fibre reinforcement. These cylinders were then subjected to a common autofrettage pressure of 400 bar, and strains developed at this pressure, together with strains permanently residing on release of pressure,

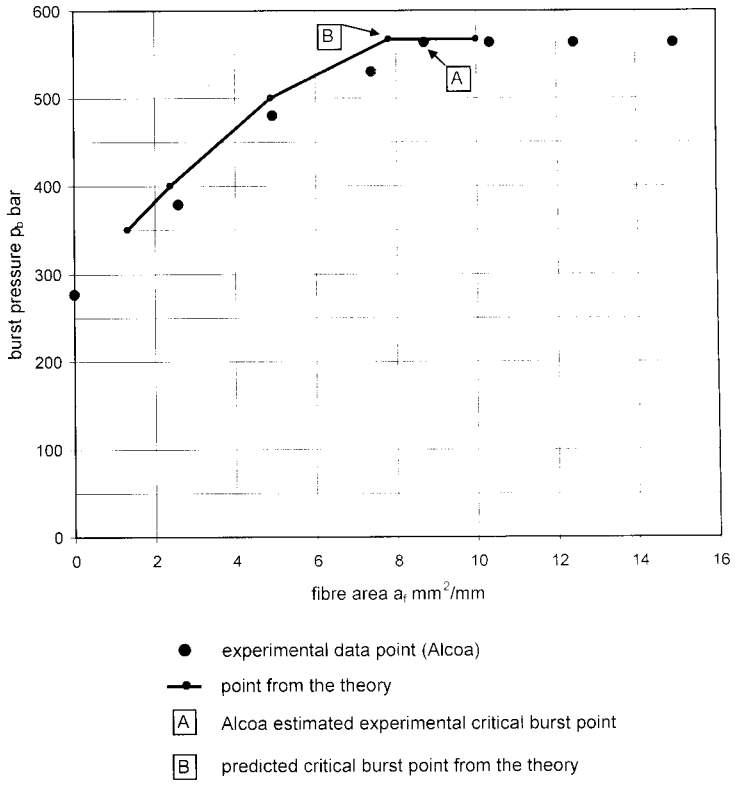

Fig. 2.2 Comparison of prediction from the theory with experimental results for cylinder bursting

were measured by strain gauges bonded onto the cylinder surfaces. In this section strains recorded in the Alcoa experiments are compared with those derived from the theory, the latter evaluation invoking in the process wide use of many of the theoretical formulae, and therefore being generally instructive in application of the theory.

2.1.3.1 Experimental results

Table 2.1 gives hoop and longitudinal strains measured by Teply and Herbein for cylinders carrying the stated

Table 2.1 Experimental strains in autofrettage – Alcoa

Cylinder number	Auto-frettage pressure (bar)	Fibre area a_f (mm^2/mm)	Total strain at autofrettage (%)		Residual strain at zero pressure (%)	
			Hoop	Longitudinal	Hoop	Longitudinal
1	400	5.41	1.30	0.40	0.75	0.25
2	400	8.29	0.85	0.38	0.40	0.13
3	400	10.81	0.60	0.20	0.20	0.08

(converted) fibre areas, all autofrettaged at 400 bar. These data are taken from Figs 9 and 10 of the Alcoa paper. As to be expected, highest strains occur with lowest reinforcement.

Note
A review of burst results in Section 2.1.2, summarized in Fig. 2.2, reveals that the reinforcement of cylinder 1 would give hoop burst, that of cylinder 2 would give more or less critical burst, and that of cylinder 3 longitudinal burst.

2.1.3.2 Theoretical results

The theory developed in Sections 1.7.2 and 1.7.3 is employed, using successive approximation to establish current yield stress at autofrettage pressure. However, because this theory is intentionally written for the usual case of deducing autofrettage pressure required to give prescribed elastic design performance in terms of pre-stress, it is necessary to modify the order of calculation. The situation is explained by reference to simplified analogy Fig. 1.6, where the usual 'design approach' task is to extrapolate the prescribed line *b* beyond point 2 on the initial yield locus

to locate point 3 on the current yield locus. However, in the case of the experimental Alcoa cylinder, autofrettage pressure is pre-fixed at 400 bar, meaning that longitudinal stress σ_l is also pre-fixed, and therefore the task is to extrapolate along this constant σ_l line to intersect stress path $1 \rightarrow 3$ at a point analogous to $2'$.

As observed in Section 2.1.3.1, only Alcoa cylinder 1 would meet the hoop burst requirement for cylinders in service, developing strains typical of the latter. Therefore, since the theoretical calculation process is essentially the same for all three tested cylinders, in the interests of brevity only cylinder 1 is evaluated here.

There are three sequential stages to the theoretical evaluation of autofrettage for the Alcoa cylinder: firstly, deducing the current strain-hardened yield stress of the liner at the prescribed autofrettage pressure of 400 bar; secondly, evaluating stresses generated in the autofrettage pressure cycle; thirdly, determining strains developed in autofrettage. Detailed calculation procedures for each of these stages are given in the following subsections.

1. Evaluation of current yield stress developed at autofrettage

Basic data for all the Alcoa cylinders are given in Section 2.1.1.

For the autofrettaged cylinder of interest, fibre area $a_f = 5.41\,\text{mm}^2/\text{mm}$.

From Section 2.1.1, derived data includes: $A = t/D = 0.0386$, $d = (D - 2t) = 304.7\,\text{mm}$, $K = d^2/(D^2 - d^2) = 5.73$.

Liner stress coefficient Z in the expression associated with equations (1.15) and (1.17) evaluates from the above data to $Z = 10.06$.

Fibre stress coefficient X in the expression associated with equation (1.18) evaluates from the above data (including Z) to $X = 8.90$.

From equation (1.22), putting $Y_0 = 276\,\text{MPa}$, initial yield pressure $p_{y0} = 298\,\text{bar}$.

Principal liner stresses associated with p_{y0} are; $\sigma_\theta = Z \cdot p_{y0} = 299.8\,\text{MPa}$, $\sigma_l = K \cdot p_{y0} = 170.8\,\text{MPa}$, $\sigma_r = -17.1\,\text{MPa}$ from equation (1.1).

All the above data are common to the following yield stress evaluation at autofrettage.

The evaluation procedure is to first assume a representative value for Y at p_a and then confirm by analysis that the assumption was valid. A key step in the procedure is adaptation of the theory developed in Section 1.4 for hoop bursting into a more general form for deducing liner hoop stress σ_θ and associated fibre stress σ_f in the pressure range $p_{y0} < p < p_b$, i.e. corresponding to prescribed $p_a = 400\,\text{bar}$. Having evaluated σ_θ and σ_f at p_a, equations (1.17) and (1.18) are used to deduce associated pre-stresses $\sigma_{\theta 0}$ and σ_{f0}, respectively, and these provide the means of solving equation (1.23) for plastic hoop strain $\varepsilon_{\theta p}$, and hence *equivalent* strain ε_{ep} and a validating yield stress Y for comparison with the starting assumed value. Calculation commences by initially assuming that Y takes the value of Y_0 (as though the liner is non-strain-hardening) and proceeds in rounds until Y from the round reconciles with that assumed at the start of the round. In the following worked evaluation three rounds of calculation are necessary to arrive at a valid current yield stress.

First approximation to yield stress, assuming $Y = Y_0 =$ 276 MPa

(i) Adapting equation (1.11) to autofrettage by substituting prescribed $p_a = 400$ bar for p_b, in associated expressions for m and n, gives $m = 210.4$ MPa and $n = -13.86 \times 10^3 (\text{MPa})^2$. Hence at $p_a = 400$ bar: $\sigma_\theta = 263.1$ MPa, from equation (1.11), $\sigma_l = K \cdot p_a = 229.2$ MPa, $\sigma_r = -28.3$ MPa from equation (1.1).

(ii) Adapting equation (1.12) to autofrettage by substituting: σ_f for T_f, a_f = prescribed5.41 mm^2/mm for a_{fb}, $p_a = 400$ bar for p_b; and putting $\sigma_0 = 263.1$ MPa from (i); transposition gives $\sigma_f = 1012.7$ MPa.

(iii) Transposing equation (1.17) for σ_{00}, and putting $\sigma_\theta = 263.1$ MPa from (i) when $p = p_a = 400$ bar, gives, $\sigma_{\theta 0} = -139.3$ MPa.

(iv) Transposing equation (1.18) for σ_{f0}, and putting $\sigma_f = 1012.7$ MPa from (ii) when $p = p_a = 400$ bar, gives, $\sigma_{f0} = 656.7$ MPa.

(v) From equation (1.23) liner plastic hoop strain $\varepsilon_{\theta p} = 1.08$ percent at p_a.

(vi) Thus liner mean stresses over the strain increment of pressure $p_{y0} \rightarrow p_a$ are, from common data stresses at p_{y0} (above) and (i): $\sigma_{\theta m} = 281.5$ MPa, $\sigma_{lm} = 200$ MPa, $\sigma_{rm} = -22.7$ MPa, and $Y_m = 276$ MPa $(= Y_0)$.

(vii) Putting $\varepsilon_{\theta p}$ from (v) in equation (1.24) liner *equivalent* plastic strain $\varepsilon_{ep} = 1.55$ percent.

(viii) Substituting this value of ε_{ep} in the tensile stress–strain model, $Y = 324[0.85 + 5(\varepsilon_{ep}) - 41.7(\varepsilon_{ep})^2]$, gives $Y = 297$ MPa. Since $Y = 297$ MPa is significantly different from the initially assumed $Y = 276$ MPa, a further round of calculation is necessary commencing with $Y = 297$ MPa.

Second approximation to yield stress, assuming $Y = 297$ MPa

(i) Adapting equation (1.11) to autofrettage by substituting prescribed $p_a = 400$ bar for p_b, in associated expressions for m and n, gives $m = 210.4$ MPa and $n = -26.36 \times 10^3$ (MPa)^2. Hence at $p_a = 400$ bar: $\sigma_\theta = 298.7$ MPa, from equation (1.11); $\sigma_l = K \cdot p_a = 229.2$ MPa; $\sigma_r = -26.9$ MPa, from equation (1.1).

(ii) Adapting equation (1.12) to autofrettage by substituting: σ_f for T_f, a_f = prescribed 5.41 mm^2/mm for a_{fb}, $p_a = 400$ bar for p_b; and putting $\sigma_\theta = 298.7$ MPa from (i); transposition gives $\sigma_f = 844.9$ MPa.

(iii) Transposing equation (1.17) for $\sigma_{\theta 0}$, and putting $\sigma_0 = 298.7$ MPa from (i) when $p = p_a = 400$ bar, gives, $\sigma_{\theta 0} = -103.7$ MPa.

(iv) Transposing equation (1.18) for σ_{f0}, and putting $\sigma_f = 844.9$ MPa from (ii) when $p = p_a = 400$ bar, gives, $\sigma_{f0} = 488.9$ MPa.

(v) From equation (1.23) liner plastic hoop strain $\varepsilon_{\theta p} = 0.80$ percent at p_a.

(vi) Thus liner mean stresses over the strain increment of pressure $p_{y0} \rightarrow p_a$ are, from common data stresses at p_{y0} (above) and (i): $\sigma_{\theta m} = 299.3$ MPa, $\sigma_{lm} = 200$ MPa, $\sigma_{rm} = -22.0$ MPa, and $Y_m = [(276 + 297)/2]$ MPa $= 286.5$ MPa.

(vii) Putting $\varepsilon_{\theta p}$ from (v) in equation (1.24), liner *equivalent* plastic strain $\varepsilon_{ep} = 1.09$ percent.

(viii) Substituting this value of ε_{ep} in the tensile stress/strain model: $Y = 324[0.85 + 5(\varepsilon_{ep}) - 41.7(\varepsilon_{ep})^2]$, gives $Y = 291.5$ MPa. Since $Y = 291.5$ MPa is significantly different from the assumed $Y = 297$ MPa,

a further round of calculation is necessary, commencing with $Y = 291.5$ MPa.

Third approximation to yield stress, assuming $Y = 291.5$ MPa

(i) Adapting equation (1.11) to autofrettage by substituting prescribed $p_a = 400$ bar for p_b, in associated expressions for m and n, gives $m = 210.4$ MPa and $n = -23.0 \times 10^3$ (MPa)^2. Hence at $p_a = 400$ bar: $\sigma_\theta = 289.8$ MPa, from equation (1.11), $\sigma_l = K \cdot p_a = 229.2$ MPa, $\sigma_r = -27.3$ MPa from equation (1.1).

(ii) Adapting equation (1.12) to autofrettage by substituting: σ_f for T_f, a_f = prescribed 5.41 mm^2/mm for a_{fb}, $p_a = 400$ bar for p_b; and putting $\sigma_\theta = 289.8$ MPa from (i); transposition gives $\sigma_f = 886.9$ MPa.

(iii) Transposing equation (1.17) for $\sigma_{\theta 0}$, and putting $\sigma_\theta = 289.8$ MPa from (i) when $p = p_a = 400$ bar, gives, $\sigma_{\theta 0} = -112.6$ MPa.

(iv) Transposing equation (1.18) for σ_{f0}, and putting $\sigma_f = 886.9$ MPa from (ii) when $p = p_a = 400$ bar, gives, $\sigma_{f0} = 530.9$ MPa.

(v) From equation (1.23) liner plastic hoop strain $\varepsilon_{\theta p} = 0.87$ percent at p_a.

(vi) Thus liner mean stresses over the strain increment of pressure $p_{y0} \rightarrow p_a$ are, from common data stresses at p_{y0} (above) and (i): $\sigma_{\theta m} = 294.8$ MPa, $\sigma_{lm} = 200$ MPa, $\sigma_{rm} = -22.2$ MPa, and $Y_m = [(276 + 291.5)/2]$ MPa $= 283.8$ MPa.

(vii) Putting $\varepsilon_{\theta p}$ from (v) in equation (1.24) liner *equivalent* plastic strain $\varepsilon_{ep} = 1.20$ percent.

(viii) Substituting this value of ε_{ep} in the tensile stress/strain model: $Y = 324[0.85 + 5(\varepsilon_{ep}) - 41.7(\varepsilon_{ep})^2]$, gives $Y = 293$ MPa.

Since this value of Y is close to that from the second approximation, $Y = 293\,\text{MPa}$ is taken as the strain-hardened yield stress resulting from autofrettage at 400 bar.

2. *Evaluation of post-autofrettage elastic stresses ($Y = 293\,MPa$)*

(i) Adapting equation (1.11) to autofrettage by substituting prescribed $p_a = 400\,\text{bar}$ for p_b, in associated expressions for m and n, gives $m = 210.4\,\text{MPa}$ and $n = -23.91 \times 10^3\,(\text{MPa})^2$. Hence at $p_a = 400\,\text{bar}$: $\sigma_\theta = 292.2\,\text{MPa}$, from equation (1.11), $\sigma_l = K \cdot p_a = 229.2\,\text{MPa}$, $\sigma_r = -27.2\,\text{MPa}$ from equation (1.1).

(ii) Adapting equation (1.12) to autofrettage by substituting: σ_f for T_f, a_f = prescribed $5.41\,\text{mm}^2/\text{mm}$ for a_{fb}, $p_a = 400\,\text{bar}$ for p_b; and putting $\sigma_\theta = 292.2\,\text{MPa}$ from (i); transposition gives $\sigma_f = 875.6\,\text{MPa}$.

(iii) Transposing equation (1.17) for $\sigma_{\theta 0}$, and putting $\sigma_\theta = 292.2\,\text{MPa}$ from (i) when $p = p_a = 400\,\text{bar}$, gives, $\sigma_{00} = -110.4\,\text{MPa}$.

(iv) Transposing equation (1.18) for σ_{f0}, and putting $\sigma_f = 875.6\,\text{MPa}$ from (ii) when $p = p_a = 400\,\text{bar}$, gives, $\sigma_{f0} = 519.6\,\text{MPa}$.

(v) Thus, over the pressure range $0 < p < 400\,\text{bar}$, the general post-autofrettage stress–pressure relationships are:

- For the liner

$$\sigma_\theta = 10.06p - 110.4\,\text{MPa} \quad \text{from equation (1.17)}$$

$$\sigma_l = K \cdot p = 5.73p$$

$$\sigma_r = -0.57p - 4.26\,\text{MPa} \quad \text{from equations (1.1) and (1.17)}$$

- For the fibre

$$\sigma_f = 8.90p + 519.6\,\text{MPa from equation (1.18)}$$

Von Mises *equivalent stress* in the liner at any pressure is found from equation (1.21).

3. Evaluation of strains in autofrettage

Procedures given in Section 1.8.4 are followed.

Although in general liner strains are given by the algebraic sum of plastic and elastic strain components, hoop strains are more conveniently evaluated in terms of fibre stresses, invoking the liner/fibre hoop strain equality condition. Thus, applying equation (1.26) at $p = p_a = 400$ bar, where $\sigma_f = 875.6$ MPa from evaluation *2* above, gives total hoop strain to autofrettage $\sigma_{0t} = 1.21$ percent. Applying equation (1.26) at $p = 0$, where $\sigma_f = \sigma_{f0} = 519.6$ MPa from evaluation *2* above, gives total residual hoop strain $\varepsilon_{00} = 0.72$ percent.

Longitudinal liner strain evaluation is less straightforward, requiring the summing of plastic and elastic components, the former being obtained in terms of plastic hoop strain $\varepsilon_{\theta p}$ as follows:

Liner mean stress values over the strain increment of pressure $p_{y0} \rightarrow p_a$ are, from common data stresses at p_{y0} (above) and evaluation *2*, step (i): $\sigma_{\theta m} = 296.0$ MPa, $\sigma_{lm} = 200$ MPa, $\sigma_{rm} = -22.2$ MPa, and $Y_m = [(276 + 293)/2]$ MPa $= 284.5$ MPa.

Applying equation (1.23), with pre-stresses σ_{00} and σ_{f0} from evaluation *2*, liner plastic hoop strain induced by autofrettage $\varepsilon_{\theta p} = 0.85$ percent.

Hence, applying equation (1.30) liner plastic longitudinal strain from autofrettage $\varepsilon_{lp} = 0.26$ percent.

Selecting the pre-autofrettage zero pressure point as the origin for liner elastic strain calculation, where

$p = 0, \sigma_\theta = 0, \sigma_l = 0, \sigma_r = 0$: longitudinal elastic strain ε_{le} at autofrettage ($p_a = 400$ bar) is given by equation (1.29), inserting stresses directly from evaluation *2*, steps (i) or (v). Thus, $\varepsilon_{le} = 0.22$ percent, and total strain $\varepsilon_{lt} = \varepsilon_{lp} + \varepsilon_{le} = 0.48$ percent. Similarly, longitudinal elastic strain ε_{le} post-autofrettage ($p = 0$) is given by equation (1.29), inserting stresses from evaluation *2*, step (v). Thus, $\varepsilon_{le} = 0.05$ percent, and total residual strain $\varepsilon_{l0} = \varepsilon_{lp} + \varepsilon_{le} = 0.31$ percent.

2.1.3.3 Comparison of theoretical and experimental autofrettage strains

Table 2.2 shows strain comparisons for cylinder 1, giving total (elastic + plastic) strains at the autofrettage conditioning pressure, and total residual strains on release of that pressure to zero, for hoop and longitudinal directions. Theory underestimates hoop strain at autofrettage by about 7 percent, and at subsequent zero pressure by about 4 percent. Longitudinal strains, which are around one-third of corresponding hoop strains, are 20 percent overestimated by the theory compared with measured values. One possible explanation for the latter difference may be the theoretical idealization of the *equivalent* stress–strain curve to a sharp elastic/plastic transition, which would be expected to reflect greater proportional effect at lower strains. Another factor could simply be author reading error in taking small strains from the Alcoa graphs. Suffice it to say that theory predicts longitudinal strains to a correct order of magnitude. From a practical aspect the most important strain in autofrettage is residual hoop strain $\varepsilon_{\theta 0}$, because of its close relationship to installed liner/fibre pre-stresses, and theory appears to predict this strain with good accuracy.

Table 2.2 Comparison of experimental and theoretical strains over autofrettage cycle for Alcoa cylinder number 1

Strain identity	*Experimental (%)*	*Theoretical (%)*
Total hoop at $p = p_a$	1.30	1.21
Residual hoop at $p = 0$	0.75	0.72
Total longitudinal at $p = p_a$	0.40	0.48
Residual longitudinal at $p = 0$	0.25	0.31

Total fibre area a_f, 5.41 mm^2/mm; autofrettage pressure p_a, 400 bar.

These results, when taken with those for burst evaluations in Section 2.1.2, demonstrate that the developed theoretical techniques in general, and those for establishing strain hardening in particular, produce reasonably reliable answers.

2.2 Cylinder design from a basic specification

In this section the theory is applied following the usual route for designing a hoop-wrapped cylinder, starting with basic parameters, such as liner/fibre materials and their associated mechanical properties, pressure duty of the cylinder including service and burst safety-requirements, together with any other safety-related influences on the design.

The design procedure is illustrated by considering a cylinder of basic specification similar to the Alcoa cylinder used for comparisons in Section 2.1, as follows:

2.2.1 Cylinder details

2.2.1.1 Liner

- Material: aluminium alloy 6061.
- Mechanical properties:
  - yield stress, 276 MPa;
  - tensile strength, 324 MPa;
  - tensile modulus, 69×10^3 MPa;
  - Poisson's ratio, 0.3.
- External diameter: 330.2 mm.

2.2.1.2 Fibre

- Material: E glass.
- Mechanical properties:
  - tensile strength (impregnated strand), 1724 MPa;
  - tensile modulus, 72.4×10^3 MPa.
- Stress ratio: 2.5 (=tensile strength/stress at service pressure).

2.2.1.3 Pressure duty

- Nominal service pressure p_s: 207 bar.
- Hydrostatic test pressure p_h: 311 bar ($=1.5p_s$).
- Minimum burst pressure p_{br}: 517 bar ($=2.5p_s$).

2.2.1.4 Additional considerations

Some design specifications require that minimum burst pressure for the *unwrapped* liner shall not be less than a prescribed proportion of the wrapped cylinder service or test pressure as a safety precaution against fibre damage/loss. While this does not affect application of the design theory, it does impose a parallel requirement on liner wall

thickness, and will therefore be taken into consideration in the following design exercise. For this purpose the widely used condition $p_{bl} \geq 0.85p_h$ will be applied.

2.2.2 Evaluation of liner wall thickness

Burst optimization theory of Section 1.5.1 describes three different burst pressures that need to be considered as part of design, namely p_{br}, p_{bd}, and p_{bc}, where $p_{bl} < p_{bd} < p_{bc}$. *Required* minimum burst pressure p_{br} is given by the specification as 517 bar. *Critical* burst pressure p_{bc}, once set relative to p_{br}, governs liner wall thickness, and *design* burst pressure p_{bd} ensures that the correct amount of fibre reinforcement is applied to result in a hoop burst mode. As stated in Section 1.5.1, the margin between these different burst pressures will depend on design/manufacturing control confidence. However, for the present exercise let it be assumed that *critical* burst pressure is designated as 110 percent of *required* minimum burst pressure; then, $p_{bc} = 569$ bar.

Liner wall thickness is found using this prescribed p_{bc} in equation (1.9), but since current yield stress Y at *critical* burst is unknown because of strain-hardening, solution follows the procedure of Section 1.9.3.1, first conducting a conditional evaluation on the basis of an assumed current yield stress value, and then by subsequent analysis confirming that the assumption was correct. In the following worked calculations, steps (i), (ii), and (iii) cover the basic *critical* burst evaluation, and steps (iv) to (x) inclusive cover validation of the initially assumed yield stress.

At the critical burst condition *equivalent* plastic straining of the liner is expected to be of the same order as that at instability in simple tension. Therefore for a first

approximation current yield stress of the liner is assumed equal to tensile strength.

The tensile stress–strain model for the liner material is (see Section 2.1.2.2)

$$Y = 324[0.85 + 5(\varepsilon_{ep}) - 41.7(\varepsilon_{ep})^2]$$

(i) Assuming $Y = T_l = 324\,\text{MPa}$ for first approximation, equation (1.9) gives $A = 0.0387$ via the numerical method recommended in Section 1.3.3.2, after equation (1.9). Hence for prescribed $D = 330.2\,\text{mm}$, $t = A \cdot D = 12.78\,\text{mm}$, $d = (D - 2t) = 304.6\,\text{mm}$, and $K = d^2/(D^2 - d^2) = 5.71$.

(ii) Principal liner stresses at p_{bc} are, following the evaluation procedure recommended in Section 1.3.3.2, after equation (1.9): $\sigma_l = K \cdot p_{bc} = 324.9$ MPa, σ_r from equation (1.6) $= -49\,\text{MPa}$, σ_θ from equation (1.7) $= 149\,\text{MPa}$.

(iii) From equation (1.10), putting $\sigma_\theta = 149\,\text{MPa}$ from (ii), fibre area for critical burst $a_{fc} = 7.84\,\text{mm}^2/\text{mm}$.

(iv) Applying equation (1.31), using stresses from (ii), liner plastic hoop strain $\varepsilon_{\theta p} = 2.3$ percent to failure at p_{bc}.

(v) Evaluating liner stress coefficient Z in the expression associated with equation (1.15), $Z = 9.39$.

(vi) Applying $Z = 9.39$ in equation (1.22), liner initial yield pressure $p_{y0} = 315.5\,\text{bar}$.

(vii) Evaluating liner principal stresses at p_{y0}: $\sigma_\theta = Z \cdot p_{y0} = 296.3\,\text{MPa}$, $\sigma_l = K \cdot p_{y0} = 180.2\,\text{MPa}$, $\sigma_r = -18.9\,\text{MPa}$ from equation (1.1).

(viii) From (ii) and (vii) liner mean stresses over the strain increment corresponding to $p_{y0} \rightarrow p_{bc}$ are therefore: $\sigma_{\theta m} = 222.7\,\text{MPa}$, $\sigma_{lm} = 252.6\,\text{MPa}$, $\sigma_{rm} = -34.0$ MPa, and $Y_m = [(276 + 324)/2]\,\text{MPa} = 300\,\text{MPa}$.

(ix) Putting $\varepsilon_{\theta p}$ from (iv) in equation (1.24), liner *equivalent* plastic strain $\varepsilon_{ep} = 6.1$ percent.

(x) From the tensile stress–strain model above, at $\varepsilon_{ep} = 6.1$ percent, $Y = 324\,\text{MPa}$, and hence the first approximation result of wall thickness = 12.78 mm is confirmed as correct.

Result:

- Liner wall thickness $t = 12.78\,\text{mm}$ for a critical burst pressure of 569 bar [and for information fibre reinforcement area to give $p_{bc} = 7.84\,\text{mm}^2/\text{mm}$ (total both sides)].

Note 1
If Y from step (x) had been found to be less than the initially assumed T_1, steps (i) to (x) would be repeated using this lower Y value. The outcome would be a larger wall thickness.

Note 2
The prescribed value of $p_{bc} = 1.10 p_{br}$ selected in this design exercise has coincidentally given a p_{bc} almost identical to that evaluated theoretically for the manufactured Alcoa cylinder (see Section 2.1.2.2, evaluation *1*). Consequently, the wall thickness emerging from this design exercise is almost identical to that of the Alcoa cylinder. Clearly, if a different prescribed value of p_{bc} had been used, the coincidence would not have arisen.

2.2.2.1 Investigation of additional requirement $p_{bl} \geq 0.85 p_h$

Since $p_h = 311$ bar, minimum liner burst pressure according to this requirement is $p_{bl} \geq 264$ bar. Referring to Annex 2, the 'Mean Diameter' burst formula (equation A2.1) would require for this burst pressure a liner wall

thickness of

$$t = \frac{330.2 \times 26.4}{(2 \times 1.09 \times 324 + 26.4)} = 11.9\,\text{mm}$$

and the von Mises based formula [equation (A2.2)], solved numerically, using mean yield stress $= (276 + 324)/2$ MPa requires a liner wall thickness of

$$t = 12.1\,\text{mm}$$

As supporting evidence, it is known from the Alcoa test results (Fig. 2.1) that a liner of wall thickness $t = 12.75$ mm gave a burst pressure around 276 bar, and this would pro rata indicate a thickness of 12.2 mm for a burst pressure of 264 bar.

Therefore from the above, it seems that the liner burst requirement gives a wall thickness just (5 percent) less than the 12.78 mm set by the critical burst design condition $p_{bc} = 1.10 p_{br}$ and thus the latter overrides.

It is beyond the scope of this design theory to enter into debate on safety factors set by regulatory or standards bodies, but in so far as calculations to the theory are concerned, clearly if the liner burst requirement *had* given a wall thickness greater than that from p_{bc} as a percentage of p_{br}, then p_{bc} would need to be re-evaluated from equation (1.9) accordingly.

2.2.3 Evaluation of fibre reinforcement area

Having designated $p_{bc} = 1.10 p_{br}$, it seems reasonable to set *design* burst pressure p_{bd} midway between these two pressures. Therefore $p_{bd} = (p_{br} + p_{bc})/2 = 1.05 p_{br} =$ 543 bar.

Fibre area required to give this *design* burst is found using theory of Section 1.5.2, applying equations (1.11a)

and (1.12a), but since liner current yield stress Y at p_{bd} is initially unknown because of strain-hardening, solution follows the procedure of Section 1.9.3.2, using the wall thickness established in Section 2.2.2, i.e. $t = 12.78$ mm, giving $A = 0.0387$, $K = 5.71$, and $d = 304.6$ mm.

The procedure involves first a conditional evaluation on the basis of an assumed current yield stress, the latter being confirmed by subsequent analysis. In the following worked calculations, steps (i) and (ii) cover the basic fibre area evaluation, and steps (iii) to (ix) inclusive cover validation of the assumed yield stress. Two rounds of calculation are used to arrive at a correct solution, although, as will be seen, the result from the first round is sufficient to provide a good estimate.

The tensile stress–strain model is, as previously (see Section 2.1.2.2)

$$Y = 324[0.85 + 5(\varepsilon_{ep}) - 41.7(\varepsilon_{ep})^2]$$

For a first approximation, liner current yield stress at *design* burst p_{bd} is assumed to be that already established (in Section 2.2.2) at p_{bc}, i.e. $Y = 324$ MPa, since p_{bd} is within 5 percent of p_{bc}.

(i) With respect to equation (1.11a), associated expressions for constants m and n give, $m = 284.5$ MPa and constant $n = 10.49 \times 10^3 (\text{MPa})^2$. Hence, liner principal stresses at burst are: $\sigma_\theta = 241.0$ MPa from equation (1.11a), $\sigma_l = K \cdot p_{bd} = 310.1$ MPa, $\sigma_r = -42.9$ MPa from equation (1.1).

(ii) From equation (1.12a), putting $\sigma_\theta = 241.0$ MPa from (i), for $p_{bd} = 543$ bar, fibre area $a_{fd} = 6.02\,\text{mm}^2/\text{mm}$.

(iii) From equation (1.31), liner plastic hoop strain $\varepsilon_{\theta p} = 2.15$ percent to hoop failure at p_{bd}.

(iv) Evaluating liner stress coefficient Z from the expression associated with equation (1.15), $Z = 9.86$.

(v) Applying $Z = 9.86$ from (iv) in equation (1.22) liner initial yield pressure $p_{y0} = 303.2$ bar.

(vi) Evaluating liner principal stresses at p_{y0}: $\sigma_\theta = Z \cdot p_{y0} = 299.0$ MPa, $\sigma_l = K \cdot p_{y0} = 173.1$ MPa, $\sigma_r = -17.6$ MPa from equation (1.1).

(vii) From (i) and (vi) mean liner stresses over the strain increment corresponding to $p_{y0} \rightarrow p_{bd}$ are therefore: $\sigma_{\theta m} = 270.0$ MPa, $\sigma_{lm} = 241.6$ MPa, $\sigma_{rm} = -30.3$ MPa, and $Y_m = [(276 + 324)/2] = 300$ MPa.

(viii) Putting $\varepsilon_{\theta p}$ from (iii) in equation (1.24) liner *equivalent* plastic strain $\varepsilon_{ep} = 3.92$ percent.

(ix) From the tensile stress–strain model, at $\varepsilon_{ep} = 3.92$ percent, $Y = 318.1$ MPa. This is within 2 percent of assumed $Y = 324$ MPa made at the start of calculation, close enough to make an informed estimate that true $Y \approx 320$ MPa, but to fully illustrate the calculation process a second approximation will be made.

For a second approximation, liner current yield stress at *design* burst is assumed to be that from the first approximation, i.e. 318 MPa.

(i) With respect to equation (1.11a), associated expressions for constants m and n give, $m = 284.5$ MPa and constant $n = 14.46 \times 10^3$ (MPa)^2. Hence, liner principal stresses at burst are: $\sigma_\theta = 218.2$ MPa from equation (1.11a), $\sigma_l = K \cdot p_{bd} = 310.1$ MPa, $\sigma_r = -43.8$ MPa from equation (1.1).

(ii) From equation (1.12a), putting $\sigma_\theta = 218.2$ MPa from (i), for $p_{bd} = 543$ bar, fibre area $a_{fd} = 6.36\,\text{mm}^2/\text{mm}$.

(iii) From equation (1.31), liner plastic hoop strain $\varepsilon_{\theta p} = 2.18$ percent to hoop failure at p_{bd}.

(iv) Evaluating liner stress coefficient Z from the expression associated with equation (1.15), $Z = 9.79$.

(v) Applying $Z = 9.79$ from (iv) in equation (1.22) liner initial yield pressure $p_{y0} = 305.0$ bar.

(vi) Evaluating liner principal stresses at p_{y0}: $\sigma_0 = Z \cdot p_{y0} = 298.6$ MPa, $\sigma_l = K \cdot p_{y0} = 174.2$ MPa, $\sigma_r = -17.8$ MPa from equation (1.1).

(vii) From (i) and (vi) mean liner stresses over the strain increment corresponding to $p_{y0} \rightarrow p_{bd}$ are therefore: $\sigma_{\theta m} = 258.4$ MPa, $\sigma_{lm} = 242.2$ MPa, $\sigma_{rm} = -30.8$ MPa, and $Y_m = [(276 + 318)/2] = 297$ MPa.

(viii) Putting $\varepsilon_{\theta p}$ from (iii) in equation (1.24), liner *equivalent* plastic strain $\varepsilon_{ep} = 4.24$ percent.

(ix) From the tensile stress–strain model, at $\varepsilon_{ep} = 4.24$ percent, $Y = 319.8$ MPa. Hence Y is confirmed at 320 MPa at *design* burst pressure $p_{bd} = 543$ bar.

2.2.3.1 Final calculation for fibre area at design burst

Having established that the liner current yield stress at design burst is $Y = 320$ MPa, it now remains to conduct a final evaluation of fibre area using this value. With respect to equation (1.11a), associated expressions for constants m and n give, $m = 284.5$ MPa and $n = 13.13 \times 10^3 (\text{MPa})^2$. Hence, from equation (1.11a) at $p_{bd} = 543$ bar, $\sigma_\theta = 226.5$ MPa, and using this value in equation (1.12a) gives fibre reinforcement area $a_{fd} = 6.24\,\text{mm}^2/\text{mm}$ (total both sides).

2.2.4 Evaluation of design stresses

Having designed liner wall thickness and fibre area, theory of Sections 1.6.2 and 1.6.3 is applied to evaluate design stresses, starting with pre-stresses.

The definitive value of liner stress coefficient Z is calculated from the expression associated with equations (1.15) and (1.17) for $t = 12.78\,\text{mm}$ and $a_{fd} = 6.24\,\text{mm}^2/\text{mm}$. Thus $Z = 9.80$.

The definitive value of fibre stress coefficient X is calculated from the expression associated with equation (1.18), using $Z = 9.80$, to give $X = 8.67$.

Equation (1.19) is solved applying the prescribed fibre stress ratio (FSR) = 2.5 at a design pressure p_d equal to service pressure $p_s = 207\,\text{bar}$ (see Section 2.2.1.2), giving a fibre pre-stress $\sigma_{f0} = 510.1\,\text{MPa}$.

Substituting this value of σ_{f0} in equation (1.20) gives liner pre-stress $\sigma_{\theta 0} = -124.5\,\text{MPa}$.

Permanent diameter expansion δD required to produce these pre-stresses is given by equation (1.25) as $\delta D = 2.3\,\text{mm}$. (The autofrettage pressure required to give these pre-stresses and expansion is deduced in Section 2.2.5).

The complete definitive stress–pressure relationships in the elastic range of cylinder operation are therefore given by:

- For the liner

$$\sigma_\theta = 9.80p - 124.5\,\text{MPa} \quad \text{from equation (1.17)}$$

$$\sigma_l = 5.71p\,\text{MPa} \quad (\sigma_l = K \cdot p)$$

$$\sigma_r = -0.58p - 4.8\,\text{MPa} \quad \text{from equations (1.1) and (1.17)}$$

- For the fibre

$$\sigma_f = 8.67p + 510.1\,\text{MPa} \quad \text{from equation (1.18)}$$

From a cyclic fatigue aspect it is interesting to evaluate liner/fibre stresses at specified hydrostatic test pressure $p_h = 311\,\text{bar}$, thus, putting $p = p_h$ in the above

$$\sigma_{fh} = 779.7\,\text{MPa}$$

$$\sigma_{\theta h} = 180.3\,\text{MPa}$$

$\sigma_{lh} = 177.6\,\text{MPa}$

$\sigma_{rh} = -22.8\,\text{MPa}$

From equation (1.21) this combination of liner stresses produces a von Mises *equivalent stress* σ_e of 201.8 MPa which equals 73 percent of Y_0, a level very similar to that accepted in all-metal industrial gas cylinders. (Autofrettage increases Y above Y_0 and thereby effectively reduces this percentage further).

2.2.5 Evaluation of autofrettage pressure

The procedure is visualized by reference to simplified analogy Fig. 1.6. Liner pre-autofrettage stress line *a* and post-autofrettage stress line *b* are both defined (see Section 2.2.4). Initial yield point 1 on line *a* is readily established via equation (1.22), but autofrettage 'conditioning' point 3, for the strain-hardened liner is unresolved because current yield stress Y at the point is initially unknown. However, point 2 on line *b* corresponding to initial yield stress Y_0 *can* be established, and this therefore is the starting point for calculation.

The procedure described in Section 1.7.3 is followed, drawing on theory developed in Sections 1.7.1, 1.7.2, and 1.7.3. Design constants already established are: $A = 0.0387$, $K = 5.71$, $Z = 9.80$, $X = 8.67$, $\sigma_{\theta 0} = -124.5\,\text{MPa}$, $\sigma_{f0} = 510.1\,\text{MPa}$. The tensile stress/strain model for the liner is, as previously: $Y = 324[0.85 + 5(\varepsilon_{cp}) - 41.7(\varepsilon_{cp})^2]$ (see Section 2.1.2.2).

2.2.5.1 Basic calculations

(i) Liner initial yield p_{y0} is given by equation (1.22) putting $Y_0 = 276\,\text{MPa}$. Thus, $p_{y0} = 304.7\,\text{bar}$.

(ii) Liner stresses at p_{y0} are: $\sigma_0 = 298.6\,\text{MPa}$ from equation (1.15), $\sigma_l = K \cdot p_{y0} = 174.0\,\text{MPa}$, $\sigma_r = -17.7\,\text{MPa}$ from equation (1.1).

(iii) Liner plastic hoop strain $\varepsilon_{\theta p}$ is given by equation (1.23) as, $\varepsilon_{0p} = 0.86$ percent (noting that this is a constant quantity defined by the elastic stress/pressure characteristics, irrespective of the magnitude of current yield stress).

(iv) Writing liner principal stresses generally in terms of pressure from Section 2.2.4, the principal stress differences are: $(\sigma_\theta - \sigma_l) = (4.09p - 124.5)\,\text{MPa}$; $(\sigma_l - \sigma_r) = (6.29p + 4.8)\,\text{MPa}$; $(\sigma_r - \sigma_\theta) = (-10.38p + 119.7)\,\text{MPa}$; and the sum of the squares of these differences is $164.03p^2 - 3443p + 29851$. It follows that:

(v) At autofrettage pressure p_a, von Mises yield criterion (1.2) is represented by

$$2Y^2 = 164.03p_a^2 - 3443p_a + 29851$$

or

$$2Y^2/164.03 = p_a^2 - 20.99p_a + 182$$

This is the general form of the quadratic for establishing autofrettage pressure p_a at current strain-hardened yield stress Y.

However, since Y is initially unknown, the procedure for fixing p_a involves first a conditional evaluation on the basis of an assumed yield stress, the latter being confirmed by subsequent analysis. In the following worked calculation, steps (i) and (ii) cover the basic autofrettage pressure and related stress evaluation, and steps (iii), (iv), and (v) cover validation of the assumed yield stress. Two rounds of calculation are necessary to arrive at a correct solution.

The starting point is to initially assume that Y at autofrettage $= Y_0$.

2.2.5.2 *Evaluating yield stress at autofrettage*

1. *First approximation to autofrettage pressure, putting* $Y = Y_0 = 276\ MPa$

(i) Solving the quadratic gives $p_a = 397.7$ bar.
(ii) Liner stresses at $p_a = 397.7$ bar are from Section 2.2.4: $\sigma_\theta = 265.2$ MPa, $\sigma_l = 227.1$ MPa, $\sigma_r = -27.9$ MPa.
(iii) Over the strain increment corresponding to $p_{y0} \rightarrow p_a$, liner mean stresses are, from (ii) and Section 2.2.5.1, step (ii), above: $\sigma_{0m} = 281.9$ MPa, $\sigma_{lm} = 200.6$ MPa, $\sigma_{rm} = -22.8$ MPa, $Y_m = Y_0 = 276$ MPa.
(iv) Hence, from equation (1.24), liner *equivalent* plastic strain increment $\sigma_{ep} = 1.43\varepsilon_{\theta p} = 1.23$ percent, where $\varepsilon_{\theta p}$ is given by Section 2.2.5.1, step (iii), above.
(v) From the tensile stress–strain model, $\varepsilon_{ep} = 1.23$ percent gives a corresponding $Y = 293.3$ MPa. This value is sufficiently larger than the assumed $Y = 276$ MPa to warrant a second approximation.

2. *Second approximation to autofrettage pressure, putting* $Y = 293.3\ MPa$

(i) Solving the quadratic gives $p_a = 417.5$ bar.
(ii) Liner stresses at $p_a = 417.5$ bar are from Section 2.2.4: $\sigma_\theta = 284.7$ MPa, $\sigma_l = 238.4$ MPa, $\sigma_r = -29.0$ MPa.
(iii) Over the strain increment corresponding to $p_{y0} \rightarrow p_a$, liner mean stresses are, from (ii) and Section 2.2.5.1, step (ii), above: $\sigma_{0m} = 291.7$ MPa, $\sigma_{lm} = 206.2$ MPa, $\sigma_{rm} = -23.4$ MPa, $Y_m = [(276 + 293.3)/2]$ MPa $= 284.7$ MPa.

(iv) Hence, from equation (1.24), liner *equivalent* plastic strain increment $\varepsilon_{ep} = 1.42\ \varepsilon_{\theta p} = 1.22$ percent where $\varepsilon_{\theta p}$ is given by Section 2.2.5.1, step (iii), above.

(v) From the tensile stress–strain model, $\varepsilon_{ep} = 1.22$ percent gives a corresponding $Y = 293.1$ MPa. This value is virtually identical to that assumed, therefore *$Y = 293$ MPa is the strain-hardened yield stress at autofrettage.*

2.2.5.3 Final calculations

Substituting $Y = 293$ MPa in the quadratic confirms autofrettage pressure at 417 bar, this being the pressure to produce the required elastic stresses in the designed cylinder.

Cylinder stresses at autofrettage pressure p_a are, from Section 2.2.4

$$\sigma_\theta = 284.2\ \text{MPa}$$
$$\sigma_l = 238.1\ \text{MPa}$$
$$\sigma_r = -29.0\ \text{MPa}$$
$$\sigma_f = 871.6\ \text{MPa}$$

The permanent diametrical expansion produced by autofrettage is $\delta D = 2.3$ mm (see Section 2.2.4).

2.2.6 Summary of cylinder design results from application of the theory

The following design results apply to the cylinder with basic specification given in Section 2.2.1.

- Design wall thickness = 12.78 mm.
  (To meet a *critical* burst pressure of 569 bar = 110 percent of *required* minimum burst pressure). (The theoretical fibre reinforcement area to give *critical* burst being 7.84 mm^2/mm total both sides.)

- Design fibre reinforcement area = 6.24 mm^2/mm total both sides.
  (To give a *design* burst pressure of 543 bar = 105 percent of *required* minimum burst pressure.)
- Generalized post-autofrettage stress expressions in pressure range $0 \leq p \leq$ autofrettage pressure.
  - Liner
    Hoop stress, $\sigma_\theta = 9.80p - 124.5$ MPa
    Longitudinal stress, $\sigma_l = 5.71p$ MPa
    Mean radial wall stress, $\sigma_r = -0.58p - 4.8$ MPa
  - Fibre
    Axial stress, $\sigma_f = 8.67p + 510.1$ MPa
- Autofrettage pressure necessary to give required pre-stresses = 417 bar.
  (Permanent diameter expansion of liner resulting from autofrettage = 2.3 mm.)
- Particular post-autofrettage stresses at key pressures are given in Table 2.3.

Table 2.3 Post-autofrettage stresses at key pressures

Stress identity	*Zero pressure, p = 0*	*Service pressure, p = 207 bar*	*Test pressure, p = 311 bar*	*Autofrettage pressure, p = 417 bar*
Hoop σ_θ (MPa)	−124.5	78.4	180.3	284.2
Longitudinal σ_l(MPa)	0	118.2	177.6	238.1
Radial σ_r (MPa)	−4.8	−16.8	−22.8	−29.0
Equivalent σ_e (MPa)(liner)	122.2	120.2	201.8	292.9
Fibre axial σ_f (MPa)	510.1	689.6	779.7	871.6

2.3 General comments

The explicit nature of the developed formulae linking the process variables enables design execution from various entry points, giving the design theory broad flexibility of use. This is evident in the different adaptation used in Section 2.1 when comparing theory with experiment, to that used in Section 2.2 when designing from basics. This adaptability, together with the transparent cause–effect relationships self-evident in the formulae, provide the design engineer with a comprehensive philosophy for understanding the mechanical behaviour of the hoop-wrapped cylinder.

An important general point arising from application of the design theory is that results are specific to the prescribed input data on liner and fibre, and also to their interaction. This applies to wall thickness, fibre area, pre-stresses, autofrettage pressure, and everything else emerging from the design exercise. A direct consequence of this is that the design parameters should be treated as actual, not minimum, values in the manufactured cylinder. This is in contrast to the approach followed in manufacturing an all-metal cylinder where it is necessary to respect only minimum design values. A secondary consequence is that best results in exploiting this theory will be obtained where manufacturing process control is tight, so that product variations are minimal. While the theory can be usefully employed to study and reveal effects of variability in the manufactured cylinder, it cannot directly influence these variables.

A particular issue arising from this general point is the effect of liner wall eccentricity on the behaviour under pressure of the composite cylinder. It is clear that with a metallic cylinder, eccentricity on any transverse plane

will be accommodated by progressive change in wall stress to satisfy the condition of constant pressure loading per unit length of circumference. However, for a composite cylinder the situation is less clear, depending on the support provided by the fibre. Two basically different conditions could be postulated. In the first, the fibre is free to slide within its resin tunnel, such that fibre tensile stress is uniform around the liner circumference, and commensurate with average hoop strain of the liner. In the second condition, the fibre is locked to the liner by the resin and therefore experiences local effects of liner hoop straining which will vary inversely with liner wall thickness. As a consequence fibre tensile stress would vary around the circumference. Such a condition could be accommodated by shear forces at the fibre/resin interface, augmented by fibre coil friction effects, especially with typical maximum levels of eccentricity (circa ± 10 percent) expected in liners, and to the author this appears the more probable of the two postulates. Accordingly, it would be appropriate to apply theory concerned with cylinder bursting to the thinnest part of the liner, as though the liner was this thickness at all points. However, for designing liner/fibre pre-stresses and associated autofrettage pressure it would be more appropriate to consider the average situation as given by the liner mean wall.

There is a general point concerning the effect on critical burst pressure of liner plastic strain development. Critical burst pressure is a key part of the design theory because it defines liner wall thickness, as given by equation (1.9), where it is seen that liner current yield stress influences the outcome. For any given liner, current yield stress at critical burst depends on the amount of strain-hardening, and hence on the amount of plastic strain developed in

pressurizing to burst. It follows from equation (1.9) that the thinnest liner meeting a given critical burst will be that where the overwrapped *fibre* permits greatest strain development prior to fracture. This in turn leads to the (at first sight surprising) conclusion that use of a stiffer fibre may, by limiting strain development, require a *thicker* liner to meet a given critical burst pressure. In other words, it should not be taken as a foregone conclusion that the use of a stiffer fibre automatically leads to a thinner liner.

In reviewing Sections 2.1 and 2.2 it will be seen that much of the calculation is taken in evaluating current strain-hardened yield stress Y, so that a true representative value of the latter may be used in the theoretical formula of interest. The procedure for establishing Y involves successive approximation. Irrespective of the calculation method used (discussed below), it is worthwhile observing the underlying mechanics of the procedure, which tend to be obscured by the volume of generated data.

In solving the autofrettage condition, successive approximation starts by assuming current yield stress Y is the initial liner yield stress Y_0, in the knowledge that plastic strain in autofrettage will generally give values for Y closer to Y_0 than tensile strength T_1. The effect of assuming a 'weak' liner is to cause calculation to overestimate plastic straining for a given applied pressure, and hence produce an *overestimate* of true yield stress from the tensile curve. Conversely, in the succeeding round of calculation this overly 'strong' cylinder from the preceding round strains less than the true cylinder, and therefore gives an *underestimate* of true yield stress, but at a value greater than initial yield stress Y_0. Thus the process successively 'homes in' on the true required value of Y.

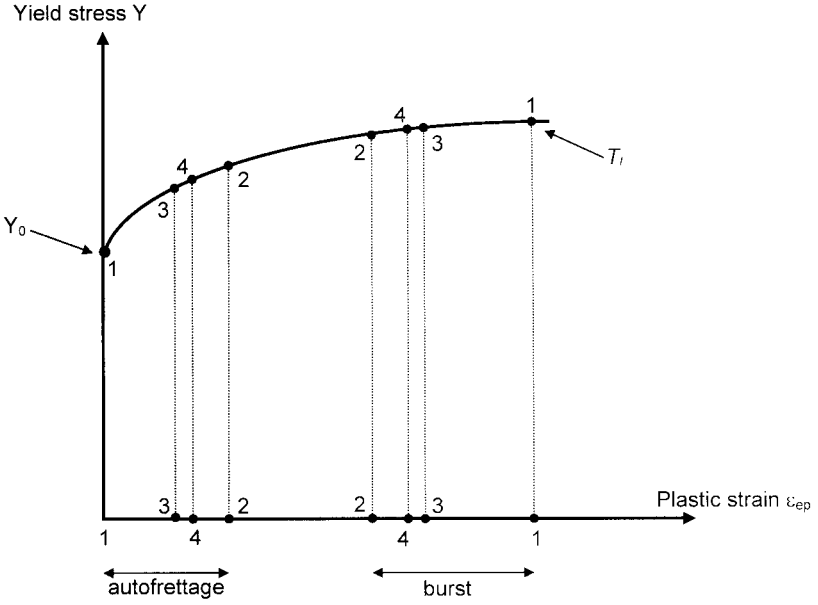

Fig. 2.3 Successive approximation to liner current yield stress at autofrettage and burst

In solving the burst condition, successive approximation starts by assuming current yield stress Y is equal to tensile strength T_l, in knowledge that plastic strain in bursting will generally give Y closer to T_l than Y_0. The calculation process follows a pattern exactly opposite to that described for autofrettage above, giving first an underestimate, and then an overestimate less than T_l, and so on.

The two successive approximation processes described above are illustrated in Fig. 2.3.

Note
With experience in using the theory for a particular combination of liner/fibre materials, and applying similar design ratios, it may be possible to make a sufficiently

accurate estimate of yield stress at autofrettage and burst without the need for successive approximation.

All design calculations carried out in Section 2 were by 'smart' calculator, mainly with the object of testing techniques, but also to prove that the theory could be applied without the need for a computer. However, this said, there is no doubt that the use of spreadsheet programmes, plugging in formulae from the theory, would greatly reduce the calculation burden, especially in the case of successive approximation. This aspect is left with the theory user.

Reference

(1) **Teply, J.L. and Herbein, W.C.** Failure modes for filament wound aluminium natural gas cylinders (Alcoa Labs, Alcoa Center, Pennsylvania). Paper presented at an ASM International Conference on *Fatigue, Corrosion Cracking, Fracture Mechanics and Failure Analysis*, Salt Lake City, Utah, December 1985.

Annexes

Annex 1

Explicit closed-form expressions for principal stresses in liner at critical burst pressure

A1.1 In terms of basic parameters

$$\sigma_{1\max} = \frac{2}{\sqrt{3}} Y \left[\frac{1 - 4A(1-A)}{1-A} \right] \sqrt{1 - A + A^2}$$

$$\sigma_{\theta} = \frac{Y}{\sqrt{3}} \left[\frac{(1+A) + 4A\{(1-A)^2(2A-1) - (1-A^2)\}}{(1-A)\sqrt{1-A+A^2}} \right]$$

$$\sigma_{r} = \frac{Y}{\sqrt{3}} \left[\frac{A^2\{17 - 8A(2-A)\} - 7A}{(1-A)\sqrt{1-A+A^2}} \right]$$

A1.2 In terms of critical burst pressure

$$\sigma_{l\max} = p_{bc}\left[\frac{1}{4A(1-A)} - 1\right]$$

$$\sigma_{\theta} = \frac{8Y^2}{3p_{bc}}\left[\frac{A(1+A)}{1-A}\right] - p_{bc}$$

$$\sigma_{r} = \frac{8Y^2}{3p_{bc}}\left[\frac{A^2(1+A)}{(1-A)}\right] - p_{bc}$$

Annex 2

Burst theory for unwrapped cylinder

While it is possible to derive expressions for pressure in the plastic range in terms of current yield stress, using an appropriate yield criterion and cylinder wall/diameter parameters, the prediction of burst pressure for a ductile strain-hardening metallic cylinder is quite complex, due to difficulty in predicting the point of instability where strain hardening can no longer keep pace with the reduction in wall thickness caused by expansion. It is important to recognize that the triaxial stress conditions in the cylinder are different to this in simple tension, and therefore *equivalent* strain to failure will not be the same in these two deformation processes. Generally speaking, *equivalent* strain to failure in the cylinder will be less than that in simple tension, implying that current strain-hardened yield stress will also be less than tensile strength. But conversely, because of the greater constraint on straining in the cylinder compared with simple tension, hoop stress at failure will exceed current yield stress.

Traditionally, this complexity in predicting burst from fundamental theory has been avoided by using simple semi-empirical burst formulae containing 'factors' adjusted to provide reasonable agreement with measured results. The most common of these is the so-called 'mean

diameter' formula:

$$p_b = F \cdot \frac{2tT}{(D-t)}$$

where T is tensile strength and F is an adjustment factor; the quantity $(D-t)$ being recognizable as cylinder mean wall diameter.

This formula is believed to have its roots in the Tresca maximum shear stress yield criterion, which ignores the effect on yielding of the intermediate size principal stress (in this case the longitudinal stress). According to Tresca yielding occurs when (greatest − smallest) principal stress equals the yield stress. For the unwrapped cylinder greatest stress is hoop stress $\sigma_\theta = pd/2t$, and smallest principal stress is radial through-wall stress σ_r which has a mean value $-p/2$. Thus according to Tresca

$$Y = \frac{pd}{2t} + \frac{p}{2}$$

giving

$$p = \frac{2tY}{(d+t)} = \frac{2tY}{(D-t)}$$

This expression is seen to resemble the above burst formula for p_b, except that in the latter, current yield stress Y has been upgraded to tensile strength T, and the factor F added. Both of these 'adjustments' correct the basic tendency of Tresca to underestimate the cylinder's strength due to ignoring the effect of the intermediate principal stress.

Gas cylinder industry experience indicates that for the grades of steels and aluminium alloys typically used for hoop-wrapped cylinder liners, factor F in the above burst formula is around 1.09. Thus the 'mean diameter' burst

formula becomes

$$p_b = 1.09 \frac{2tT}{(D-t)} \tag{A2.1}$$

As part of developing hoop-wrapped cylinder design theory the author considered it of interest to derive the equivalent of equation (A2.1) taking all three principal stresses into account in von Mises yield criterion, i.e. putting $\sigma_\theta = pd/2t$, $\sigma_l = pd^2/(D^2 - d^2)$, $\sigma_r = -p/2$ in

$$2Y^2 = (\sigma_\theta - \sigma_l)^2 + (\sigma_l - \sigma_r)^2 + (\sigma_r - \sigma_\theta)^2$$

After tidying by ignoring negligibly small terms, this resulted in the expression

$$p = \frac{2}{\sqrt{3}} Y \cdot \frac{2A(1-A)}{\sqrt{1-4A}} \tag{A2.2}$$

where

$$A = t/D$$

Although equation (A2.2) is likely to be more fundamentally correct than equation (A2.1), it still suffers from the same problem of not knowing current Y at the point of instability, i.e. at maximum (burst) pressure. Furthermore, equation (A2.2) is more awkward to use than equation (A2.1), especially in transposing for wall thickness. By comparing with known burst results, and also by comparing with equation (A2.1), it was found that equation (A2.2) gives reasonably accurate burst pressure prediction putting current yield stress at instability as the *mean* of initial yield stress Y_0 and tensile strength T, a result which is qualitatively consistent with known facts of the burst condition.

Annex 3

Tensile stress–strain model for estimating strain-hardened yield stress of liner

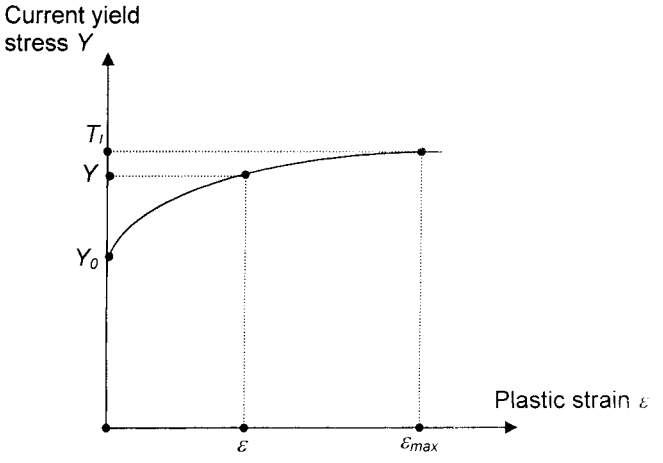

Fig. A3.1 Plastic stress–strain model

Materials used for hoop-wrapped liners are generally in a heat-treated, hardened/tempered condition for which the yield/tensile ratio is around 0.9. For these materials the plastic stress–strain curve can be approximated by the polynomial

$$Y = a + b\varepsilon + c\varepsilon^2 \tag{A3.1}$$

Where the three unknown constants a, b, c, are given by the three properties of the curve

$$Y = Y_0 \qquad \text{when } \varepsilon = 0$$

$$Y = T_1 \qquad \text{when } \varepsilon = \varepsilon_{max}$$

$$dY/d\varepsilon = 0 \qquad \text{when } \varepsilon = \varepsilon_{max}$$

Applying these conditions to equation (A3.1) results in

$$a = Y_0$$
$$b = 2(T_1 - Y_0)/\varepsilon_{max}$$
$$c = -(T_1 - Y_0)/(\varepsilon_{max})^2$$

Substituting the above values for a, b, c, into equation (A3.1), and writing $Y_0/T_1 = x$, provides the final expression

$$Y = T_1\left[x + \left\{\frac{2(1-x)}{\varepsilon_{max}}\right\}\varepsilon - \left\{\frac{1-x}{\varepsilon_{max}^2}\right\}\varepsilon^2\right] \qquad \text{(A3.2)}$$

Note
The model is valid for equivalent plastic strain $\varepsilon \leq \varepsilon_{max}$. (For $\varepsilon > \varepsilon_{max}$, $Y \geq T_1$.)

Index

Designing high-pressure gas cylinders using composites is a relatively new and rapidly developing technology, exploiting recent advances in high-strength, lightweight synthetic fibres. Traditionally, only metals have been used, but clearly weight is a major consideration in the efficiency of gas cylinders. Lightweight composite cylinders offer considerable advantages over heavier all-metal alternatives, provided concerns over safety can be allayed.

Manufacture of composite gas cylinders has relied primarily on costly 'design by testing' to ensure that stringent safety standards are met. With new European and International Standards backed by recently introduced legislation ***Hoop-wrapped, Composite, Internally Pressurized Cylinders – Development and Application of a Design Theory*** provides the industry with a much-needed, reliable, and transparent methodology for the design of hoop-wrapped, composite gas cylinders.

This short monograph and timely practitioner guide offers a comprehensive theoretical background and a design procedure for hoop-wrapped, composite gas cylinders. It gives a fundamental insight into the effects of process variables and how they interact, allowing a predictive approach to design and enabling test results to be assessed in a more meaningful way. The theory described is also generally applicable to all kinds of internally pressurized cylindrical pressure vessels and pipes where hoop reinforcement is an integral part of the design.

Hoop-wrapped, Composite, Internally Pressurized Cylinders will be invaluable to professional practitioners involved in cylinder design, manufacture, use, inspection, certification, and safety regulation. Some of the fundamental concepts explained also overlap with the broader field of general pressure vessel research.

Consultant ***John A Walters***, BSc, PhD has a career spanning over 45 years in the industry, first with the Tube Investments Group and Chesterfield Cylinders in the UK, and latterly with the US company Norris Cylinders. He has contributed to numerous British, European, and International Standards workshops and committees relating to gas cylinder design – and was awarded the BSI Distinguished Service Certificate in 2002. His main objective is that this book will be openly available to all as a primary text, and his hope is that it will be adopted as an unofficial design standard, bringing much needed transparency and harmonization to the industry.

ISBN 1-86058-425-X

9 781860 584251

Professional Engineering Publishing